FEDERAL RESERVE BANK
PHILADELPHIA

Working Papers
RESEARCH DEPARTMENT

Are Fiscal Transfers Inflationary?

Jonas E. Arias
Federal Reserve Bank of Philadelphia

Juan F. Rubio-Ramírez
Emory University, Federal Reserve Bank of Atlanta, and Visiting Scholar, Federal Reserve Bank of Philadelphia Research Department

Minchul Shin
Federal Reserve Bank of Philadelphia

WP 26-23

PUBLISHED
May 2026

ISSN: 1962-5361

DOI: https://doi.org/10.21799/frbp.wp.2026.23

Are Fiscal Transfers Inflationary?

Jonas E. Arias
Federal Reserve Bank of Philadelphia

Juan F. Rubio-Ramírez*
Emory University
Federal Reserve Bank of Atlanta

Minchul Shin
Federal Reserve Bank of Philadelphia

April 9, 2026

Abstract

We assess the inflationary effects of fiscal transfers by leveraging advances in the identification of fiscal policy shocks within the recently proposed rotation-invariant time-varying structural vector autoregression. Our analysis suggests that fiscal transfer shocks account for a sizable share of the early post-pandemic increase in the price level through mid-2021. Thereafter, the rise in the price level is dominated by adverse supply shocks (especially supply-chain disruptions), while demand shocks mainly matter later for the lift-off in short-term interest rates. In addition, we find that fiscal transfers were essential for preventing a decline in real output per capita similar to the one experienced during the Great Depression.

JEL classification: C11, C51, E62
Keywords: fiscal policy, structural vector autoregressions, identification.

The views expressed in this paper are solely those of the authors and do not necessarily reflect the views of the Federal Reserve Bank of Atlanta, the Federal Reserve Bank of Philadelphia, or the Federal Reserve System. Any errors or omissions are the responsibility of the authors.

*Corresponding author: Juan F. Rubio-Ramírez <juan.rubio-ramirez@emory.edu>, Economics Department, Emory University, Rich Memorial Building, Room 306, Atlanta, Georgia 30322-2240. We thank Jesper Lindé, Maximilian Breitenlechner, and seminar participants at the Dutch National Bank, Erasmus University of Rotterdam, King's College London, and the Federal Reserve Bank of Philadelphia's Workshop on Methods and Applications for DSGE models, for helpful comments.

1 Introduction

The recent surge in U.S. inflation to levels unseen since the 1970s has triggered a broad effort to understand its underlying causes. Early commentary raised concerns that pandemic-related fiscal measures could be inflationary, while associated supply chain disruptions were also viewed as potential inflation drivers. See Cochrane (2022); Summers (2022) for early discussions of the inflationary risks of expansive fiscal policy, and Akinci et al. (2022); Powell (2021) for analyses of supply-side imbalances. A growing academic literature has since sought to decompose the contributions of broadly defined demand and supply shocks to this inflationary episode (Blanchard and Bernanke, 2023; Shapiro, 2024; Giannone and Primiceri, 2024; Bergholt et al., 2024), estimate the causal effects of supply-side shocks (di Giovanni, 2022; Bai et al., 2024), and assess the role of fiscal policy (Bianchi, Faccini and Melosi, 2023; Ascari et al., 2024).

This paper contributes to this literature by assessing the role of fiscal transfers from a novel perspective: identifying exogenous fiscal transfer shocks within a time-varying SVAR and quantifying their effects on output and prices. The focus on fiscal transfers is warranted because the bulk of the pandemic fiscal response consisted of transfers to households rather than government purchases, which makes standard spending-multiplier results less directly applicable. The fiscal expansion of 2020–2021 included the Coronavirus Aid, Relief, and Economic Security (CARES) Act, the Coronavirus Response and Relief Supplemental Appropriations Act, and the American Rescue Plan (ARP). Together, these measures amounted to approximately 11 percent of 2019 GDP—surpassed only by the fiscal expansion during World War II. Yet much of the empirical literature on fiscal policy focuses on government consumption and investment (Blanchard and Perotti, 2002; Caldara and Kamps, 2017). A notable exception is Romer and Romer (2016), who studied increases in Social Security transfers between 1952 and 1991 to assess their effects on personal consumption under permanent and temporary changes. However, their work concentrated on real outcomes and did not consider the inflationary effects of transfer shocks.

More specifically, this paper identifies the causal effects of exogenous fiscal transfers by adapting the identification strategies of Blanchard and Perotti (2002); Caldara and Kamps

(2017) to a time-varying setting. To do so, we extend the rotation-invariant time-varying structural vector autoregression (TV-SVAR) framework of Arias, Rubio-Ramirez, Shin, and Waggoner (2026) to incorporate zero restrictions. Existing heteroskedastic approaches (see, e.g., Sentana and Fiorentini, 2001; Rigobon, 2003; Lanne and Lütkepohl, 2008; Lanne, Lütkepohl and Maciejowska, 2010; Brunnermeier et al., 2021) cannot accommodate both systematic and non-systematic fiscal policy shifts, a limitation our rotation-invariant TV-SVAR with zero restrictions overcomes. This lets us account for structural change without shortening the sample and use data extending back to the early 1950s, in contrast to Blanchard and Bernanke (2023); Giannone and Primiceri (2024), who begin their estimations in the 1990s.

In addition to fiscal transfer shocks, we identify demand, cost-push, global supply chain, and monetary policy shocks, and analyze their contributions to unexpected movements in key macroeconomic variables during the Great Recession and the pandemic, and their aftermaths. Our results show that fiscal transfer shocks raise output and prices, but the magnitude of the price response depends on the systematic monetary policy reaction. During the pandemic, the monetary policy reaction to the fiscal expansion was not enough to prevent transfer shocks from fueling inflation. Instead, during the Great Recession, monetary policy responded forcefully, preventing significant price pressures, though at the cost of weaker output support.

Our analysis yields several key results. In the post-pandemic period, transfer shocks were extremely large and made a substantial contribution to real GDP per capita. Absent these transfers, real GDP per capita would have fallen by more than 20 percent—a contraction rivaling the Great Depression. This stimulus, however, came at the cost of a substantial rise in the price level. Moreover, monetary policy was accommodative, as the positive impact of transfers on yields was more than offset by demand and supply forces that drove interest rates to the lower bound. By contrast, transfer shocks during the Great Recession were modest, leaving inflation contained while output contracted sharply. To assess whether the absence of inflation simply reflected the smaller scale of the shocks, we conduct a counterfactual in which the Great Recession is replayed with transfer shocks of the pandemic's magnitude while keeping the rest of the Great Recession shocks unchanged. The results show that prices would have risen but more modestly than during the pandemic because interest rates would have increased much more. This underscores the critical role of systematic monetary policy:

because rates would have risen forcefully in response to large transfer shocks—offsetting the downward pressure from negative demand shocks—the inflationary effect of transfers would have been limited.

These findings confirm the conjecture of Romer and Romer (2016) that the macroeconomic effects of transfers hinge on the monetary policy response. Although they did not study price effects directly, they noted that the short-lived response of consumption to permanent benefit increases could plausibly be explained by tighter monetary policy, citing policy discussions in which officials viewed transfers as a reason to raise rates. Similarly, our results are qualitatively consistent with the findings of Bianchi, Faccini and Melosi (2023).

The paper proceeds as follows. Section 2 highlights the importance of fiscal transfers in the Great Recession and the pandemic. Section 3 lays out the time-varying SVAR, the identifying restrictions, the sampling algorithm, and explains why allowing for time variation is essential. Section 4 presents the main historical decomposition for the 2021–2022 inflation episode, while Section 5 presents the corresponding analysis for the Great Recession. Section 6 concludes.

2 The Overlooked Component: Fiscal Transfers

Research by McKay and Reis (2016); Angeletos, Lian, and Wolf (2024) highlights that fiscal transfers can shape output and prices, yet they remain comparatively understudied. Table 1 reports stylized facts that motivate our focus on transfers. The first column lists categories of government current expenditures (BEA NIPA Table 3.1). The second and third columns report the changes in each category over 2007–2009 and 2019–2021, respectively, using annual data—periods chosen to capture the fiscal responses to the Great Recession and the COVID-19 pandemic.

Consistent with Oh and Reis (2012), transfers to persons account for a large share of the increase in government expenditures during the Great Recession. In 2007–2009, transfers to persons accounted for about one-half of the 803.6 billion rise in total expenditures, while government purchases (consumption and gross investment) accounted for about one-third. The pandemic response was even more concentrated in transfers: in 2019–2021, transfers

Category	2007–2009	2019–2021
(a) Change (billions of dollars)		
Total Expenditures	803.6	2416.5
Transfers to Persons	410.4	1475.9
Gov. Purchases (C&I)	285.8	422.7
Subsidies	3.7	553.1
(b) Change (percent of GDP)		
Total Expenditures	5.6%	11.2%
Transfers to Persons	2.8%	6.9%
Gov. Purchases (C&I)	2.0%	2.0%
Subsidies	0.0%	2.6%

Table 1: Fiscal Responses: The Great Recession and the Pandemic

to persons accounted for about 60 percent of the 2,416.5 billion increase, while government purchases accounted for only 17 percent of that increase; transfers to persons and subsidies together exceeded 80 percent of the total. Panel (b) scales these changes by GDP.

Figure 1 places these episodes in a longer-run perspective using annual BEA data. Transfers to persons have trended upward as a share of GDP since World War II, whereas government purchases have trended downward.

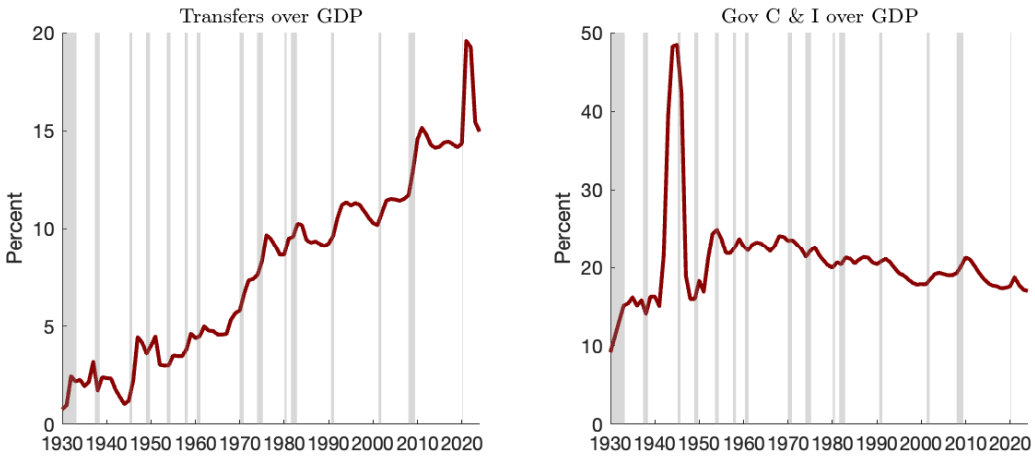

Figure 1: Transfers to Persons versus Government Purchases

Put together, these facts suggest an important gap: the fiscal literature's emphasis on multipliers from government purchases overlooks that transfers account for most of the discretionary response in the last two recessions. Some exceptions include Shapiro and

Slemrod (2003, 2009); Parker, Souleles, Johnson, and McClelland (2013); Orchard, Ramey, and Wieland (2025), who estimate marginal propensities to consume from transfers, and Romer and Romer (2016), who study the impact of Social Security transfers on personal consumption between 1952 and 1991. However, this work largely abstracts from the effects of transfers on prices. We instead focus on the effects of exogenous transfer shocks on inflation, output, interest rates, and other macroeconomic variables during both the pandemic and the Great Recession.

3 Methodology

Identifying the causal effects of fiscal transfers requires separating exogenous policy innovations from systematic policy responses to macroeconomic conditions. Moreover, as we show in Section 3.4, the propagation of shocks and the variances of structural disturbances change over time. We therefore estimate the rotation-invariant time-varying SVAR introduced by Arias, Rubio-Ramirez, Shin, and Waggoner (2026). Section 3.1 describes the model, Section 3.2 describes the data, model specification, and identifying restrictions, and Section 3.3 describes the sampling algorithm (which can be skipped by readers primarily interested in the empirical results).

3.1 The Model

Following Bognanni (2018); Arias, Rubio-Ramirez, Shin, and Waggoner (2026), we consider a rotation-invariant time-varying SVAR in structural form:

$$\mathbf{y}_t' \mathbf{A}_t = \mathbf{x}_t' \mathbf{F}_t + \boldsymbol{\varepsilon}_t' \text{ with } \boldsymbol{\varepsilon}_t \sim \mathrm{N}(\mathbf{0}_n, \mathbf{I}_n) \text{ for } 1 \leq t \leq T, \tag{1}$$

where $\mathbf{y}_t$ is an $n \times 1$ vector of endogenous variables and $\mathbf{x}_t = \begin{bmatrix} 1 & \mathbf{y}_{t-1}' & \cdots & \mathbf{y}_{t-p}' \end{bmatrix}'$ collects a constant and p lags (so $m = np + 1$). The shocks $\boldsymbol{\varepsilon}_t$ are orthogonal structural innovations, normalized to have identity covariance, and the time-varying structural parameters are the invertible $n \times n$ matrix $\mathbf{A}_t$ and the $m \times n$ matrix $\mathbf{F}_t$. Initial conditions $(\mathbf{y}_0, \cdots, \mathbf{y}_{1-p})$ are unrestricted. We complement (1) with a rotation-invariant prior over the time-varying structural parameters that will be implicitly defined below.

Equivalently, the model can be parameterized in terms of time-varying reduced-form parameters $(\mathbf{B}_t, \mathbf{\Sigma}_t)_{t=1}^T$ and a sequence of time-varying orthogonal matrices $(\mathbf{Q}_t)_{t=1}^T$, in which case (1) can be written as follows:

$$\mathbf{y}_t' = \mathbf{x}_t' \mathbf{B}_t + \boldsymbol{\varepsilon}_t' \mathbf{Q}_t' h(\mathbf{\Sigma}_t) \text{ for } 1 \leq t \leq T, \tag{2}$$

where $h(\mathbf{\Sigma})$ is any differentiable matrix decomposition satisfying $h(\mathbf{\Sigma})' h(\mathbf{\Sigma}) = \mathbf{\Sigma}$ and $(\mathbf{Q}_t)_{t=1}^T \in \mathcal{O}_n^T$. Here, $\mathcal{O}_n$ denotes the set of all $n \times n$ orthogonal matrices and $\mathcal{O}_n^T = \prod_{t=1}^T \mathcal{O}_n$ denotes the set of all length-T sequences of $n \times n$ orthogonal matrices. We take h to be the upper triangular Cholesky decomposition, normalized so that the diagonal is positive, though any differentiable decomposition suffices.

The orthogonal reduced-form parameters can be turned into structural parameters by exploiting the following invertible mapping from the time-varying structural parameters to the time-varying orthogonal reduced-form parameters:

$$f_h((\mathbf{A}_t, \mathbf{F}_t)_{t=1}^T) = \Big(\underbrace{\mathbf{F}_t \mathbf{A}_t^{-1}}_{\mathbf{B}_t}, \underbrace{(\mathbf{A}_t \mathbf{A}_t')^{-1}}_{\mathbf{\Sigma}_t}, \underbrace{h((\mathbf{A}_t \mathbf{A}_t')^{-1}) \mathbf{A}_t}_{\mathbf{Q}_t} \Big)_{t=1}^T.$$

Following Archakov and Hansen (2021), we map $\mathbf{\Sigma}_t$ to $(\boldsymbol{\delta}_t, \boldsymbol{\gamma}_t) \in \mathbb{R}^n \times \mathbb{R}^{n_\gamma}$, where $n_\gamma = n(n-1)/2$, and define an invertible function $g((\mathbf{B}_t, \mathbf{\Sigma}_t, \mathbf{Q}_t)_{t=1}^T) = (\mathbf{B}_t, \boldsymbol{\delta}_t, \boldsymbol{\gamma}_t, \mathbf{Q}_t)_{t=1}^T$. This mapping provides the flexibility to model the evolution of the time-varying reduced-form covariance matrix via random walk processes. Our algorithm draws from $(\mathbf{B}_t, \boldsymbol{\delta}_t, \boldsymbol{\gamma}_t, \mathbf{Q}_t)_{t=1}^T$ and uses $(g \circ f_h)^{-1}$ to map these orthogonal reduced-form parameters into their structural form representation. We assume the following law of motion for $(\mathbf{B}_t, \boldsymbol{\delta}_t, \boldsymbol{\gamma}_t)_{t=2}^T$:

$$\boldsymbol{\beta}_t = \boldsymbol{\beta}_{t-1} + \boldsymbol{\nu}_t, \text{ with } \boldsymbol{\nu}_t \sim \mathrm{N}(\mathbf{0}_{nm}, \mathbf{V}_{\boldsymbol{\beta}}) \text{ and } \boldsymbol{\beta}_t = \mathrm{vec}(\mathbf{B}_t), \tag{3}$$

$$\boldsymbol{\delta}_t = \boldsymbol{\delta}_{t-1} + \boldsymbol{\eta}_t, \text{ with } \boldsymbol{\eta}_t \sim \mathrm{N}(\mathbf{0}_n, \mathbf{V}_{\boldsymbol{\delta}}), \tag{4}$$

$$\boldsymbol{\gamma}_t = \boldsymbol{\gamma}_{t-1} + \boldsymbol{\zeta}_t, \text{ with } \boldsymbol{\zeta}_t \sim \mathrm{N}(\mathbf{0}_{n_\gamma}, \mathbf{V}_{\boldsymbol{\gamma}}), \tag{5}$$

where $\mathbf{V}_{\boldsymbol{\beta}}$ is an $nm \times nm$ symmetric positive definite matrix, $\mathbf{V}_{\boldsymbol{\delta}} = \mathrm{diag}(V_{\delta,1}, \ldots, V_{\delta,n})$ is an $n \times n$ diagonal matrix with positive entries, and $\mathbf{V}_{\boldsymbol{\gamma}} = \mathrm{diag}(V_{\gamma,1}, \ldots, V_{\gamma,n_\gamma})$ is an $n_\gamma \times n_\gamma$ diagonal matrix with positive entries. We also assume $\boldsymbol{\beta}_1 \sim \mathrm{N}(\mathbf{m}_{\boldsymbol{\beta}_1}, \mathbf{V}_{\boldsymbol{\beta}_1})$, where $\mathbf{m}_{\boldsymbol{\beta}_1}$ is a

$nm \times 1$ vector and $\mathbf{V}_{\boldsymbol{\beta}_1}$ is an $nm \times nm$ symmetric positive definite matrix; $\boldsymbol{\delta}_1 \sim \mathrm{N}(\mathbf{m}_{\boldsymbol{\delta}_1}, \mathbf{V}_{\boldsymbol{\delta}_1})$, where $\mathbf{m}_{\boldsymbol{\delta}_1}$ is an $n \times 1$ vector and $\mathbf{V}_{\boldsymbol{\delta}_1}$ is diagonal with positive entries; and $\boldsymbol{\gamma}_1 \sim \mathrm{N}(\mathbf{m}_{\boldsymbol{\gamma}_1}, \mathbf{V}_{\boldsymbol{\gamma}_1})$, where $\mathbf{m}_{\boldsymbol{\gamma}_1}$ is an $n_\gamma \times 1$ vector and $\mathbf{V}_{\boldsymbol{\gamma}_1}$ is diagonal with positive entries. It is straightforward to see that the constant parameters of the model are:

$$\boldsymbol{\phi} = (\mathrm{vech}(\mathbf{V}_{\boldsymbol{\beta}}), \mathrm{diag}(\mathbf{V}_{\boldsymbol{\delta}}), \mathrm{diag}(\mathbf{V}_{\boldsymbol{\gamma}}), \mathbf{m}_{\boldsymbol{\beta}_1}, \mathrm{vech}(\mathbf{V}_{\boldsymbol{\beta}_1}), \mathbf{m}_{\boldsymbol{\delta}_1}, \mathrm{diag}(\mathbf{V}_{\boldsymbol{\delta}_1}), \mathbf{m}_{\boldsymbol{\gamma}_1}, \mathrm{diag}(\mathbf{V}_{\boldsymbol{\gamma}_1}))\,.$$

Equations (3)-(5) imply a prior over $(\mathbf{B}_t, \boldsymbol{\delta}_t, \boldsymbol{\gamma}_t)_{t=1}^T$ that we denote by $p((\mathbf{B}_t, \boldsymbol{\delta}_t, \boldsymbol{\gamma}_t)_{t=1}^T \mid \boldsymbol{\phi})$. We combine this prior with the uniform prior over the sequence of time-varying orthogonal matrices in order to induce a rotation-invariant prior over the time-varying structural parameters, denoted by $p((\mathbf{A}_t, \mathbf{F}_t)_{t=1}^T \mid \boldsymbol{\phi})$.[1] Together with a prior $p(\boldsymbol{\phi})$, our prior over the time-varying structural parameters implies a posterior over the time-varying structural parameters that we label $p((\mathbf{A}_t, \mathbf{F}_t)_{t=1}^T, \boldsymbol{\phi} \mid (\mathbf{y}_t)_{t=1}^T)$ and can be written as

$$p((\mathbf{A}_t, \mathbf{F}_t)_{t=1}^T, \boldsymbol{\phi} \mid (\mathbf{y}_t)_{t=1}^T) = v_{(g \circ f_h)}((\mathbf{A}_t, \mathbf{F}_t)_{t=1}^T) p((\mathbf{B}_t, \boldsymbol{\delta}_t, \boldsymbol{\gamma}_t)_{t=1}^T \mid \boldsymbol{\phi}) \tag{6}$$

where $(\mathbf{B}_t, \boldsymbol{\delta}_t, \boldsymbol{\gamma}_t, \mathbf{Q}_t)_{t=1}^T = (g \circ f_h)(\mathbf{A}_t, \mathbf{F}_t)_{t=1}^T$ and the volume element is defined as $v_{(g \circ f_h)}((\mathbf{A}_t, \mathbf{F}_t)_{t=1}^T) = \prod_{t=1}^T v_{(g \circ f_h)}(\mathbf{A}_t, \mathbf{F}_t)$. Arias, Rubio-Ramirez, Shin, and Waggoner (2026) refer to the resulting model as random correlations (RC)-SVAR. The objective is to draw from the posterior defined in Equation (6), conditional on the sign and zero restrictions imposed to solve the identification problem associated with this class of structural models.

3.2 Data, Specification, and Identification

Our dataset includes government social benefits to persons (which we refer to as fiscal transfers) as a share of one-quarter-lagged nominal GDP, real output per capita (in log differences), the GDP deflator (in log differences), the 1-year Treasury yield, the ISM manufacturing supplier deliveries index, and the personal saving rate. We use quarterly data from 1953:Q2 to 2019:Q4. Data availability for the 1-year Treasury yield dictates the start date, and we end the sample in 2019:Q4 to align the starting point of our historical decomposition with

[1] A rotation-invariant prior assigns equal density under the volume measure to observationally equivalent structural parameters.

Giannone and Primiceri (2024).[2] As is typical in quarterly time-varying SVARs, we include a constant and two lags. Accordingly, $n = 6$, $p = 2$, and $m = 13$ in this model.

Our SVAR variables follow the literature, except that we focus on transfers to persons rather than government purchases (consumption and gross investment), and we include the ISM (Manufacturing) supplier deliveries index and the personal saving rate. The ISM supplier deliveries index measures delivery delays: values above 50 indicate slower deliveries and values below 50 indicate faster deliveries. We include it to capture supply chain disruptions during the post-pandemic inflation episode. We include the personal saving rate to capture households' spending-versus-saving margin in response to transfers. Following Gertler and Karadi (2015); Giannone and Primiceri (2024), we use the 1-year Treasury yield rather than the federal funds rate as the monetary policy instrument, which captures the effects of quantitative easing through its effect on short-term yields.

Appendix I describes our prior over $\boldsymbol{\phi}$. For ease of exposition, we summarize it here. We set $\mathbf{m}_{\boldsymbol{\beta}_1}$ equal to the maximum likelihood estimate of a constant-parameter reduced-form VAR—featuring the same variables, constant, and lags as our time-varying model—based on the first $T_0 = 40$ observations in our sample. We denote this estimate by $\hat{\mathbf{B}}$. We set $\mathbf{V}_{\boldsymbol{\beta}_1}$ to 4 times an unbiased estimator of the variance of $\hat{\mathbf{B}}$, as in Primiceri (2005). To set the values for $\boldsymbol{m}_{\boldsymbol{\delta}_1}$, $\boldsymbol{m}_{\boldsymbol{\gamma}_1}$, $\boldsymbol{V}_{\boldsymbol{\delta}_1}$, and $\boldsymbol{V}_{\boldsymbol{\gamma}_1}$, first we let $\hat{\boldsymbol{\Sigma}}$ denote the maximum likelihood estimate of the residual covariance matrix. Second, we use the delta method to set the values for $\boldsymbol{m}_{\boldsymbol{\delta}_1}$, $\boldsymbol{V}_{\boldsymbol{\delta}_1}$, $\boldsymbol{m}_{\boldsymbol{\gamma}_1}$, and $\boldsymbol{V}_{\boldsymbol{\gamma}_1}$. We set the variances $\boldsymbol{V}_{\boldsymbol{\delta}_1}$ and $\boldsymbol{V}_{\boldsymbol{\gamma}_1}$ equal to 4 times the variance implied by the delta method. Turning to the parameters governing the step sizes of the processes for $\boldsymbol{\beta}_t$, $\boldsymbol{\delta}_t$, and $\boldsymbol{\gamma}_t$ ($\mathbf{V}_{\boldsymbol{\beta}}$, $\mathbf{V}_{\boldsymbol{\delta}}$, and $\mathbf{V}_{\boldsymbol{\gamma}}$, respectively), we impose an Inverse-Wishart prior for $\mathbf{V}_{\boldsymbol{\beta}}$ and an Inverse-Gamma prior for each of the diagonal entries of $\mathbf{V}_{\boldsymbol{\delta}}$ and $\mathbf{V}_{\boldsymbol{\gamma}}$. We choose the scale parameters for these priors to be constant fractions of the maximum likelihood estimate variances for $\boldsymbol{\beta}$, $\boldsymbol{\delta}$, and $\boldsymbol{\gamma}$ in the constant-parameter reduced-form VAR over the training sample described above. We follow Primiceri (2005) when setting the degrees of freedom (for the Inverse-Wishart prior) and the shape parameters (for the Inverse-Gamma priors); we set them so that the priors are diffuse and uninformative.

[2] Alternatively, we could extend our data to 2025:Q2 and use the smoothed parameters for 2019:Q4 to perform our analysis.

Identification of Fiscal Transfer Shocks

We identify a fiscal transfer shock by extending the ideas of Blanchard and Perotti (2002) and Caldara and Kamps (2017). Specifically, we treat the first equation as the fiscal transfer rule and, abstracting from lagged variables and the time-varying constant term, write it as

$$\tau_t = \psi_{y,t}\Delta y_t + \psi_{p,t}\Delta p_t + \psi_{i,t} i_t + \psi_{\mathrm{d},t}\mathrm{d}_t + \psi_{\mathrm{psr},t}\mathrm{psr}_t + \sigma_{\tau,t}\varepsilon_{\tau,t},$$

where τ_t is transfers over lagged nominal GDP, Δy_t and Δp_t are log differences of real output per capita and the GDP deflator, i_t is the 1-year Treasury yield, d_t is the ISM Supplier Deliveries Index, psr_t is the personal saving rate, and $\varepsilon_{\tau,t}$ is the fiscal transfer shock. This specification captures the systematic component of fiscal policy described in Restriction 1.

Restriction 1. *Fiscal transfers react contemporaneously only to output growth. The contemporaneous reaction to output growth, $\psi_{y,t}$, is negative and bounded by $\bar{\psi}_{y,t}$. In addition, we impose positive sign restrictions on the standard deviation of the non-systematic component of government expenditures, $\sigma_{g,t} > 0$, and the contemporaneous impulse response of fiscal transfers.*

This identification scheme is motivated as follows. The assumption requiring that transfers over GDP only react contemporaneously to output growth (i.e., $\psi_{p,t} = \psi_{i,t} = \psi_{\mathrm{d},t} = \psi_{\mathrm{psr},t} = 0$) is motivated by the fact that the U.S. government has used transfers to stimulate economic activity in the last three recessions. In addition, Caldara and Kamps (2017) demonstrate empirically that simple fiscal rules of this type can serve as a good summary measure for the systematic component of fiscal policy. Restricting the sign of $\psi_{y,t}$ to be negative is motivated by the notion that transfers to persons increase when macroeconomic conditions deteriorate. For example, Giorno, Richardson, Roseveare, and van den Noord (1995) obtain negative elasticities of unemployment-related expenditure to output for all the major advanced economies included in their study. The average elasticity across all countries in their study is -0.4 and the elasticity for the U.S. is -0.2.[3] To discipline the estimation of the elasticity, inspired by Kilian and Murphy (2012), we impose an upper bound, $\bar{\psi}_{y,t}$, that is equal to 5

[3]The elasticities of current primary government expenditure to output are also negative for all countries except for the U.K. The average elasticity across countries is -0.14 and the elasticity for the U.S. is -0.1.

times the elasticity for the U.S. estimated by Giorno, Richardson, Roseveare, and van den Noord (1995). This is a conservative choice; for example, Blanchard and Perotti (2002) use Giorno et al.'s elasticity estimate directly (without the multiplier) in their influential work in the fiscal literature. Even so, our approach is flexible enough to accommodate alternative thresholds.

We base the assumption that fiscal transfers do not react to contemporaneous inflation on institutional knowledge. In particular, as documented by Romer and Romer (2016), until 1974 Social Security benefits in the United States were not automatically adjusted for cost of living. Since then, Social Security benefits have been indexed to cost of living adjustments (COLA). COLA is calculated by comparing the Consumer Price Index for Urban Wage Earners and Clerical Workers (CPI-W) averaged over July through September of the current year against the baseline period, which is the most recent year in which a COLA was implemented. For example, the 2019 COLA of 2.8% was derived by comparing the July-September 2018 CPI-W average of 246.352 against the 2017 baseline of 239.668, yielding an increase of 2.8%, resulting in automatic benefit increases for Social Security recipients beginning in January 2019. This type of indexation is partly captured by the lags of our SVAR.

Turning to the remaining sign restrictions, the positive response of fiscal transfers serves as a normalization along with the sign restriction on the standard deviation of the non-systematic component of government expenditures. Restricting the impact response of transfers avoids paradoxical cases in which the stimulus is so effective that the government undoes the expansionary transfers via its systematic component within a quarter.

Identification of the Remaining Structural Shocks

In addition to the fiscal transfers shock described above, we identify four other structural shocks by imposing sign restrictions on impulse responses (Uhlig, 2005). Table 2 displays the signs of the restricted contemporaneous impulse responses. Each column of the table represents a shock and the rows within a column represent the contemporaneous responses of each variable to the shock under analysis.

As in Giannone and Primiceri (2024), we identify a demand shock by assuming that upon impact it generates positive co-movement among output growth, inflation, and the 1-year

Treasury yield. In contrast, we identify a monetary policy shock by assuming that upon impact it induces negative co-movement between the 1-year Treasury yield, on the one hand, and output growth and inflation, on the other. Like most of the literature, we identify supply shocks by assuming that upon impact they generate negative co-movement between output growth and inflation. However, to isolate the effects of supply chain disruptions from other types of supply shocks, we deconstruct the supply shocks into two types depending on their effects on the ISM Supplier Deliveries Index: "Supply Chain Shocks" that generate negative co-movement between output growth and the ISM Supplier Deliveries Index, and "Cost-Push Shocks" that generate positive co-movement between output growth and the ISM Supplier Deliveries Index. An example of a supply chain shock is an exogenous disturbance to the global supply chain. An example of a cost-push shock could be a price mark-up shock. The rationale for deconstructing the supply shocks into two types is to provide a unique role to supply chain disruptions such as those highlighted by Benigno, di Giovanni, Groen, and Noble (2022); di Giovanni, Kalemli-Ózcan, Silva, and Yildirim (2022); Bai, Fernandez-Villaverde, Li, and Zanetti (2024).

Variables Shocks	Demand	Monetary Policy	Supply Chain	Cost-Push
Transfers over GDP				
Output Growth	+	-	-	-
Inflation	+	-	+	+
1-year Treasury yield	+	+		
ISM Supplier Deliveries Index			+	-
Personal Saving Rate				

Table 2: Structural Shocks Beyond Fiscal Transfers

Shocks are normalized so that positive fiscal transfer and demand shocks are expansionary, positive monetary policy shocks are contractionary, and positive supply chain and cost-push shocks are inflationary. The unidentified shock in our 6-variable time-varying SVAR is labeled as "Other" and it does not have an economic interpretation.

3.3 The Algorithm

The identification strategy adopted in this paper extends the rotation-invariant time-varying SVAR framework of Arias, Rubio-Ramirez, Shin, and Waggoner (2026) to accommodate

exclusion (zero) restrictions alongside sign restrictions. In this section, we present a Gibbs sampler that draws from the posterior distribution of the structural parameters, conditional on these restrictions. Sign restrictions can be imposed on all shocks in the system. The zero restrictions considered here identify a single shock by restricting one column of $\mathbf{A}_t$, which suffices for the identification scheme described in Section 3.2.[4]

Let $\mathbb{O}_S^T$ denote the set of sequences $(\mathbf{A}_t, \mathbf{F}_t)_{t=1}^T$ that satisfy the sign restrictions. Since we impose zero restrictions on only one column of $\mathbf{A}_t$, without loss of generality we order the equations and variables so that the zero restrictions correspond to the first z_t entries of the first column of $\mathbf{A}_t$. Let $\mathbb{O}_Z^T$ denote the set of sequences of $(\mathbf{A}_t, \mathbf{F}_t)_{t=1}^T$ that satisfy the zero restrictions. Equipped with these definitions, we can formally state that our objective is to sample from the posterior of $(\mathbf{A}_t, \mathbf{F}_t)_{t=1}^T$ conditional on the sign and zero restrictions

$$p((\mathbf{A}_t, \mathbf{F}_t)_{t=1}^T, \boldsymbol{\phi} \mid (\mathbf{y}_t)_{t=1}^T, \mathbb{O}_S^T, \mathbb{O}_Z^T)$$

defined as

$$\frac{p((\mathbf{y}_t)_{t=1}^T \mid (\mathbf{A}_t, \mathbf{F}_t)_{t=1}^T)\,[(\mathbf{A}_t, \mathbf{F}_t)_{t=1}^T \in \mathbb{O}_S^T]\,[(\mathbf{A}_t, \mathbf{F}_t)_{t=1}^T \in \mathbb{O}_Z^T]\,p((\mathbf{A}_t, \mathbf{F}_t)_{t=1}^T \mid \boldsymbol{\phi})p(\boldsymbol{\phi})}{\int\int_{\mathbb{O}_S^T \cap \mathbb{O}_Z^T} p((\mathbf{y}_t)_{t=1}^T \mid (\mathbf{A}_t, \mathbf{F}_t)_{t=1}^T)p((\mathbf{A}_t, \mathbf{F}_t)_{t=1}^T \mid \boldsymbol{\phi})d(\mathbf{A}_t, \mathbf{F}_t)_{t=1}^T p(\boldsymbol{\phi})d\boldsymbol{\phi}}. \quad (7)$$

The mappings between the parameterizations described in Section 3.1 (that is, $(\mathbf{B}_t, \boldsymbol{\delta}_t, \boldsymbol{\gamma}_t, \mathbf{Q}_t)_{t=1}^T = (g \circ f_h)(\mathbf{A}_t, \mathbf{F}_t)_{t=1}^T$) imply that the exclusion restrictions in our setup amount to imposing zero restrictions on the first z_t entries of the first column of $\mathbf{Q}_t$, while leaving $(\mathbf{B}_t, \boldsymbol{\delta}_t, \boldsymbol{\gamma}_t)_{t=1}^T$ unrestricted. Let $\tilde{\mathbb{O}}_S^T$ denote the set of sequences $(\mathbf{B}_t, \boldsymbol{\delta}_t, \boldsymbol{\gamma}_t, \mathbf{Q}_t)_{t=1}^T$ that satisfy the sign restrictions and let $\tilde{\mathbb{O}}_Z^T$ denote the set of sequences $(\mathbf{Q}_t)_{t=1}^T$ that satisfy the zero restrictions.

Since the objective is to sample from Equation (7), one may be tempted to instead sample from the posterior of $(\mathbf{B}_t, \boldsymbol{\delta}_t, \boldsymbol{\gamma}_t, \mathbf{Q}_t)_{t=1}^T$ conditional on the sign and zero restrictions

$$p((\mathbf{B}_t, \boldsymbol{\delta}_t, \boldsymbol{\gamma}_t, \mathbf{Q}_t)_{t=1}^T, \boldsymbol{\phi} \mid (\mathbf{y}_t)_{t=1}^T, \tilde{\mathbb{O}}_S^T, \tilde{\mathbb{O}}_Z^T)$$

[4] It is straightforward to adapt the approach to impose zero response restrictions one column of $\mathbf{L}_{0,t}$, where $\mathbf{L}_{0,t} = (\mathbf{A}_t^{-1})'$ denotes the contemporaneous impulse responses, instead of $\mathbf{A}_t$.

defined as

$$\frac{p((\mathbf{y}_t)_{t=1}^T \mid (\mathbf{B}_t, \boldsymbol{\delta}_t, \boldsymbol{\gamma}_t)_{t=1}^T)\left[(\mathbf{B}_t, \boldsymbol{\delta}_t, \boldsymbol{\gamma}_t, \mathbf{Q}_t)_{t=1}^T \in \tilde{\mathbb{O}}_S^T\right]\left[(\mathbf{Q}_t)_{t=1}^T \in \tilde{\mathbb{O}}_Z^T\right] p((\mathbf{B}_t, \boldsymbol{\delta}_t, \boldsymbol{\gamma}_t)_{t=1}^T \mid \boldsymbol{\phi}) p(\boldsymbol{\phi})}{\int \int_{\tilde{\mathbb{O}}_S^T \cap \tilde{\mathbb{O}}_Z^T} p((\mathbf{y}_t)_{t=1}^T \mid (\mathbf{B}_t, \boldsymbol{\delta}_t, \boldsymbol{\gamma}_t)_{t=1}^T) p((\mathbf{B}_t, \boldsymbol{\delta}_t, \boldsymbol{\gamma}_t)_{t=1}^T \mid \boldsymbol{\phi}) d(\mathbf{B}_t, \boldsymbol{\delta}_t, \boldsymbol{\gamma}_t, \mathbf{Q}_t)_{t=1}^T p(\boldsymbol{\phi}) d\boldsymbol{\phi}},$$

and then map $(\mathbf{B}_t, \boldsymbol{\delta}_t, \boldsymbol{\gamma}_t, \mathbf{Q}_t)_{t=1}^T$ to $(\mathbf{A}_t, \mathbf{F}_t)_{t=1}^T$ using $(g \circ f_h)^{-1}$. This is the correct approach for inference based on rotation-invariant priors when only sign restrictions are present. With zero restrictions, however, this approach is incorrect because the volume element becomes $v_{(g\circ f_h)|\mathbb{O}_Z^T}((\mathbf{A}_t, \mathbf{F}_t)_{t=1}^T) = \prod_{t=1}^T v_{(g\circ f_h)|\mathbb{O}_Z^T}(\mathbf{A}_t, \mathbf{F}_t)$ and, in general, it differs from $v_{(g\circ f_h)}((\mathbf{A}_t, \mathbf{F}_t)_{t=1}^T)$. For this reason, in the presence of zero restrictions, one must sample from the posterior

$$\frac{v_{(g\circ f_h)}((\mathbf{A}_t, \mathbf{F}_t)_{t=1}^T)}{v_{(g\circ f_h)|\mathbb{O}_Z^T}((\mathbf{A}_t, \mathbf{F}_t)_{t=1}^T)} p((\mathbf{B}_t, \boldsymbol{\delta}_t, \boldsymbol{\gamma}_t, \mathbf{Q}_t)_{t=1}^T, \boldsymbol{\phi} \mid (\mathbf{y}_t)_{t=1}^T, \tilde{\mathbb{O}}_S^T, \tilde{\mathbb{O}}_Z^T),$$

where $(\mathbf{A}_t, \mathbf{F}_t)_{t=1}^T = (g \circ f_h)^{-1}(\mathbf{B}_t, \boldsymbol{\delta}_t, \boldsymbol{\gamma}_t, \mathbf{Q}_t)_{t=1}^T$. Algorithm 1 describes a Gibbs sampler that accomplishes this objective.

Algorithm 1. *This algorithm approximates draws from* $p((\mathbf{A}_t, \mathbf{F}_t)_{t=1}^T, \boldsymbol{\phi} \mid (\mathbf{y}_t)_{t=1}^T, \mathbb{O}_S^T, \mathbb{O}_Z^T)$.

1. *Let* $I > 1$, *set* $i = 1$, *and assign initial values to* $(\boldsymbol{\delta}_t^{i-1}, \boldsymbol{\gamma}_t^{i-1}, \mathbf{Q}_t^{i-1})_{t=1}^T, \boldsymbol{\phi}^{i-1}$.

2. *Draw* $(\mathbf{B}_t^i)_{t=1}^T$ *from*

$$p((\mathbf{B}_t)_{t=1}^T \mid (\boldsymbol{\delta}_t^{i-1}, \boldsymbol{\gamma}_t^{i-1}, \mathbf{Q}_t^{i-1})_{t=1}^T, \boldsymbol{\phi}^{i-1}, (\mathbf{y}_t)_{t=1}^T, \tilde{\mathbb{O}}_S^T).$$

3. *Draw* $(\mathbf{Q}_t^i)_{t=1}^T$ *from*

$$p((\mathbf{Q}_t)_{t=1}^T \mid (\mathbf{B}_t^i, \boldsymbol{\delta}_t^{i-1}, \boldsymbol{\gamma}_t^{i-1})_{t=1}^T, \boldsymbol{\phi}^{i-1}, (\mathbf{y}_t)_{t=1}^T, \tilde{\mathbb{O}}_S^T, \tilde{\mathbb{O}}_Z^T).$$

4. *Draw* $(\boldsymbol{\delta}_t^i, \boldsymbol{\gamma}_t^i)_{t=1}^T$ *from*

$$\frac{v_{(g\circ f_h)}((\mathbf{A}_t, \mathbf{F}_t)_{t=1}^T)}{v_{(g\circ f_h)|\mathbb{O}_Z^T}((\mathbf{A}_t, \mathbf{F}_t)_{t=1}^T)} p((\boldsymbol{\delta}_t, \boldsymbol{\gamma}_t)_{t=1}^T \mid (\mathbf{B}_t^i, \mathbf{Q}_t^i)_{t=1}^T, \boldsymbol{\phi}^{i-1}, (\mathbf{y}_t)_{t=1}^T, \tilde{\mathbb{O}}_S^T),$$

where $(\mathbf{A}_t, \mathbf{F}_t)_{t=1}^T = (g \circ f_h)^{-1}(\mathbf{B}_t^i, \boldsymbol{\delta}_t, \boldsymbol{\gamma}_t, \mathbf{Q}_t^i)_{t=1}^T$.

5. *Draw* $\boldsymbol{\phi}^i$ *from*

$$p(\boldsymbol{\phi} \mid (\mathbf{B}_t^i, \boldsymbol{\delta}_t^i, \boldsymbol{\gamma}_t^i, \mathbf{Q}_t^i)_{t=1}^T, (\mathbf{y}_t)_{t=1}^T).$$

6. *Set* $(\mathbf{A}_t^i, \mathbf{F}_t^i)_{t=1}^T = (g \circ f_h)^{-1}((\mathbf{B}_t^i, \boldsymbol{\delta}_t^i, \boldsymbol{\gamma}_t^i, \mathbf{Q}_t^i)_{t=1}^T)$.

7. *If* $i < I$, *let* $i = i + 1$ *and return to Step 2.*

Two details clarify where the zero restrictions enter. First, these restrictions affect only the conditional distribution of $(\mathbf{Q}_t)_{t=1}^T$ (Step 3). Since they amount to setting the first z_t entries of the first column of $\mathbf{Q}_t$ equal to zero, conditional on $(\mathbf{Q}_t)_{t=1}^T$ the zero restrictions are independent of $(\mathbf{B}_t, \boldsymbol{\delta}_t, \boldsymbol{\gamma}_t)_{t=1}^T$. Second, the ratio of volume elements, between $v_{(g\circ f_h)}((\mathbf{A}_t, \mathbf{F}_t)_{t=1}^T)$ and $v_{(g\circ f_h)|\mathbb{O}_Z^T}((\mathbf{A}_t, \mathbf{F}_t)_{t=1}^T)$, only affects the conditional distribution of $(\boldsymbol{\delta}_t, \boldsymbol{\gamma}_t)_{t=1}^T$ (Step 4). While $v_{(g\circ f_h)}$ only depends on $(\boldsymbol{\delta}_t, \boldsymbol{\gamma}_t)_{t=1}^T$, it is easy to show that the same is true for $v_{(g\circ f_h)|\mathbb{O}_Z^T}$. This is because the derivative of the zero restrictions is a subset of rows of the identity matrix and, hence, its null space is a subset of columns of the identity matrix.

While Steps 2 and 5 match those described in Arias, Rubio-Ramirez, Shin, and Waggoner (2026), Steps 3 and 4 differ. Step 3 can be implemented by drawing from

$$\left[(\mathbf{B}_t, \boldsymbol{\delta}_t, \boldsymbol{\gamma}_t, \mathbf{Q}_t)_{t=1}^T \in \tilde{\mathbb{O}}_S^T\right] \prod_{t=1}^T p(\mathbf{Q}_t \mid \tilde{\mathbb{O}}_{Z,t}), \tag{8}$$

where $\tilde{\mathbb{O}}_{Z,t}$ denotes the set of orthogonal matrices $\mathbf{Q}_t$ that satisfy the zero restrictions in period t and $p(\mathbf{Q}_t \mid \tilde{\mathbb{O}}_{Z,t})$ is uniform over this set, for $1 \le t \le T$. Drawing from this distribution can be accomplished using the elliptical sampler described in Arias, Rubio-Ramirez, and Shin (2025) and exploiting the unit sphere parameterization in Arias, Rubio-Ramírez, and Waggoner (2018).[5] In particular, for periods in which $\mathbf{A}_t$ is restricted, let $\boldsymbol{\xi}_{1,t} \in \mathbb{R}^{n+1-j-z_t}$ and $\boldsymbol{\xi}_{j,t} \in \mathbb{R}^{n+1-j}$ for $2 \le j \le n$ be independently drawn from a standard normal distribution. Then, we can define $\mathbf{Q}_t = \begin{bmatrix} \mathbf{q}_{1,t} & \dots & \mathbf{q}_{n,t} \end{bmatrix}$ recursively by $\mathbf{q}_{j,t} = \mathbf{K}_{j,t} \frac{\boldsymbol{\xi}_{j,t}}{\|\boldsymbol{\xi}_{j,t}\|}$ for any matrix $\mathbf{K}_{j,t}$ whose columns form an orthonormal basis for the null space of the matrix

$$\mathbf{M}_{1,t} = \left[\mathbf{0}_{z,(n-z)}, \mathbf{I}_z\right] \text{ and } \mathbf{M}_{j,t} = \begin{bmatrix} \mathbf{q}_1 & \cdots & \mathbf{q}_{j-1} \end{bmatrix}' \text{ for } j = 2, \dots, n,$$

[5] Let us highlight that this implementation is more efficient than the conditionally uniform implementation in Arias, Rubio-Ramirez, and Shin (2025) and hence it can serve as to speed up in the implementation of the rotation-invariant SVARs proposed by Arias, Rubio-Ramirez, and Shin (2025).

where $\mathbf{0}_{z,(n-z)}$ is an $z \times (n-z)$ matrix of zeros. Notice that the structure of $\mathbf{M}_{1,t}$ satisfies Restriction 1. For periods in which $\mathbf{A}_t$ is not restricted, we have that $\boldsymbol{\xi}_{1,t} \in \mathbb{R}^{n+1-j}$ and $\mathbf{M}_{1,t} = \varnothing$. The derivations above define a mapping from $\boldsymbol{\Xi}_t = \begin{bmatrix} \boldsymbol{\xi}_{1,t} & \dots & \boldsymbol{\xi}_{n,t} \end{bmatrix}$ to $\mathbf{Q}_t$. We will denote such a mapping by $\mathbf{Q}_t = \gamma_t(\boldsymbol{\Xi}_t)$ and the volume element associated with such a mapping by $v_{\gamma_t}(\boldsymbol{\Xi}_t)$. Hence, if we draw $\boldsymbol{\Xi}_t$ from a distribution that has a density proportional to

$$\left[(\mathbf{B}_t, \boldsymbol{\delta}_t, \boldsymbol{\gamma}_t, \mathbf{Q}_t)_{t=1}^T \in \tilde{\mathbb{O}}_S^T\right] \prod_{t=1}^T \prod_{j=1}^n p(\boldsymbol{\xi}_{j,t}) \tag{9}$$

and set $\mathbf{Q}_t = \gamma_t(\boldsymbol{\Xi}_t)$ for $t = 1, \dots, T$, we obtain samples from the density described in Equation (8). Drawing from Equation (9) can be implemented using the elliptical sampler approach by treating

$$\left[(\mathbf{B}_t, \boldsymbol{\delta}_t, \boldsymbol{\gamma}_t, \mathbf{Q}_t)_{t=1}^T \in \tilde{\mathbb{O}}_S^T\right]$$

as the likelihood and noting that the prior over $(\boldsymbol{\Xi}_t)_{t=1}^T$ is Gaussian. Step 4 can be implemented using the elliptical sampler approach by treating

$$\left[(\mathbf{B}_t, \boldsymbol{\delta}_t, \boldsymbol{\gamma}_t, \mathbf{Q}_t)_{t=1}^T \in \tilde{\mathbb{O}}_S^T\right] \frac{v_{(g \circ f_h)}((\mathbf{A}_t, \mathbf{F}_t)_{t=1}^T)}{v_{(g \circ f_h)|\mathbb{O}_Z^T}((\mathbf{A}_t, \mathbf{F}_t)_{t=1}^T)} \prod_{t=1}^T p(\mathbf{y}_t \mid \mathbf{x}_t, \mathbf{B}, \boldsymbol{\delta}_t, \boldsymbol{\gamma}_t),$$

where $(\mathbf{A}_t, \mathbf{F}_t)_{t=1}^T = (g \circ f_h)^{-1}(\mathbf{B}_t, \boldsymbol{\delta}_t, \boldsymbol{\gamma}_t, \mathbf{Q}_t)_{t=1}^T$ as the likelihood and noting that the prior over $(\boldsymbol{\delta}_t, \boldsymbol{\gamma}_t)_{t=1}^T$ is Gaussian.

Our main results, shown in Section 4, are based on one independent chain obtained using Algorithm 1. The chain consists of 1,000,000 draws; we retain every 50th draw of the structural parameters. Of the resulting 20,000 draws, we discard the first 4,000 retained draws.

3.4 The Need for a Time-Varying SVAR

Estimating the time-varying model is computationally intensive due to the dimension of the parameter space. This may tempt one to instead use a standard (and faster) constant-parameter SVAR with conjugate priors. Even though taking the constant parameter path is appealing, parameter instability is a central concern when studying the drivers of inflation. For example, Giannone and Primiceri (2024); Blanchard and Bernanke (2023) start their

estimation in the 1990s, citing evidence of a break in inflation dynamics. In this section, we provide direct evidence that, in our model, impulse responses, systematic responses, and the variances of structural shocks vary over time.

(a) Output

(b) Price Level

(c) ISM Supplier Deliveries Index

(d) 1-Year Treasury Yield

Figure 2: Posterior impulse responses one year after a one-standard-deviation fiscal transfer shock: 30-year rolling-window constant-parameter SVARs. The solid black curves represent the point-wise posterior medians, and the gray-shaded areas represent the 68 percent equal-tailed point-wise probability bands.

To do so, we estimate a sequence of constant-parameters SVARs and compute: (i) the impulse responses of output, prices, the ISM Supplier Deliveries Index, and interest rates to a fiscal transfer shock; (ii) the systematic response of fiscal transfers to output growth; and (iii) the standard deviation of the fiscal transfer shock. We use a uniform-normal-inverse-Wishart

distribution for the priors over the orthogonal reduced-form parameterization, impose a Minnesota prior, and follow Giannone, Lenza, and Primiceri (2015) when choosing the parameter values that maximize the marginal likelihood. We use Restriction 1 to identify the fiscal transfers shock. We consider a sequence of 30-year rolling-window constant-parameters SVARs. The first SVAR in the rolling-window estimation uses data from 1953:Q2 through 1983:Q1, and the last SVAR uses data from 1990:Q1 through 2019:Q4. We obtain 10,000 posterior draws and retain one every 10th draw using the sampler of Arias, Rubio-Ramirez, and Shin (2025).

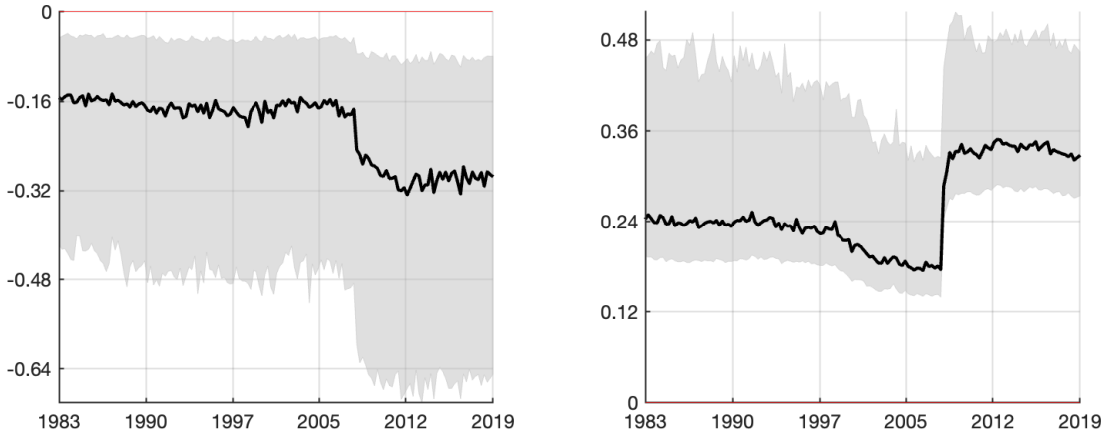

(a) Systematic Response to Output, $\psi_{y,t}$.

(b) Standard Deviation, $\sigma_{\tau,t}$.

Figure 3: Posterior distribution of the systematic response of fiscal policy to output growth and the standard deviation of the fiscal transfers shock: constant-parameters SVARs (30-year rolling window). The solid black curves represent the point-wise posterior medians, and the gray-shaded areas represent the 68 percent equal-tailed point-wise probability bands.

Figure 2 shows the impulse responses of output, the price level, the ISM Supplier Deliveries Index, and the 1-year Treasury yield one year after a fiscal transfer shock. Impulse response estimates exhibit persistence across the rolling-windows, but they also display clear changes that motivate a time-varying specification. Figure 3 reports the systematic response of fiscal transfers to output growth and the standard deviation of fiscal transfer shocks, which also exhibit noticeable time-varying patterns. Importantly, variation in $\psi_{y,t}$ implies that a model with only heteroskedastic structural shocks (see e.g., Sentana and Fiorentini, 2001; Rigobon, 2003; Lanne and Lütkepohl, 2008; Lanne, Lütkepohl and Maciejowska, 2010; Brunnermeier

et al., 2021) would not serve our purposes well; therefore, we use the rotation-invariant time-varying SVAR described in Section 3.1.

4 The Shocks Behind the 2021–22 Inflation

In the spirit of Giannone and Primiceri (2024), we conduct a historical decomposition of the U.S. economy starting in 2019:Q4 to quantify how different structural shocks contributed to the inflation surge of 2021-2022. Our analysis also speaks to whether fiscal transfers stimulate output and other macroeconomic variables (e.g., Ramey, 2025).

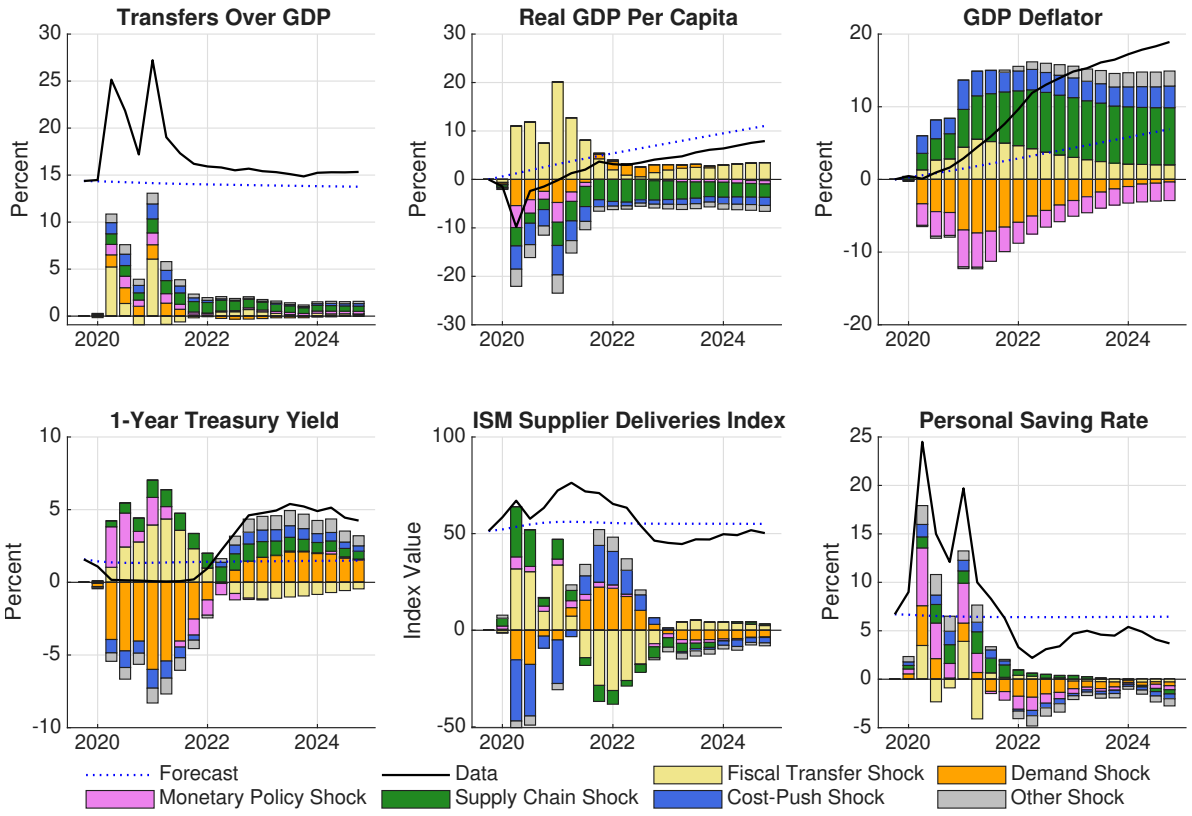

Figure 4: Time-Varying Parameters SVAR

We find that fiscal transfer shocks are pivotal in sustaining output during the early days of the COVID-19 pandemic, preventing a contraction comparable to the Great Depression, though at the cost of a significant and lasting increase in the price level. However, fiscal transfer shocks are not the main driver of inflation. Inflation is dominated primarily by supply shocks—most notably, disruptions to supply chains. Demand shocks gain relevance later,

contributing to the lift-off in interest rates, but their cumulative contribution to the price level remains negative. Monetary policy shocks are overall contractionary and contribute negatively to prices. We therefore conclude that the post-COVID inflation surge reflects expansionary fiscal policy interacting with adverse supply shocks, rather than monetary policy shocks relative to the pre-pandemic systematic component.

Figure 4 presents the posterior mean of the cumulative historical decomposition of the six variables in our SVAR for the period 2020:Q1–2024:Q4, based on the structural parameters identified in 2019:Q4.[6] The black solid lines are the data, and the dotted blue lines are the forecast from 2020:Q1 onward based on the 2019:Q4 parameters. The gaps between them represent the unpredictable evolution of the data from the perspective of the end of 2019. For each variable, the gap is decomposed into contributions from the five identified shocks and a residual category ("other"); each of these contributions is represented by a colored bar. Next, we discuss how each shock shaped the evolution of the macroeconomic variables.

Fiscal Transfer Shocks

Fiscal transfer shocks account for about half of the unexpected surge in the transfers-to-GDP ratio in both 2020:Q2 and 2021:Q1, reflecting the CARES Act and the ARP Act. This implies that the increase in transfers exceeds the endogenous systematic response by a substantial margin during these two episodes. Their effects on output are large but short-lived: although their contribution fades by the end of 2021, they contribute about 10 percentage points to the cumulative unexpected change in real GDP per capita during 2020 and slightly more than 20 percentage points after the ARP Act. Without these transfers, real GDP per capita would have fallen by more than 20 percent. The effects on prices appear later than those on output, but fiscal transfer shocks are an important and persistent positive contributor to the GDP deflator, raising the price level by roughly five percent by the end of 2021 and continuing to contribute significantly through the end of 2024. Our findings imply an important trade-off: while fiscal transfers clearly support output in the short run, they also raise prices. Thus, even though as we will discuss below supply shocks account for most of the inflation surge under analysis, fiscal transfer shocks put persistent upward pressure on the price level.

[6] Appendix III reports the posterior means along with the 68 percent probability bands.

Turning to the effects of fiscal transfer shocks on the remaining variables, they push up the 1-year Treasury yield through end-2021. This early increase in interest rates may dampen the expansionary and inflationary effects of fiscal transfer shocks and may help explain, in part, the delayed increase in prices. The fiscal transfer shocks also contribute strongly to delivery delays in 2020 and early 2021. These effects are consistent with the pronounced positive effects on GDP, suggesting that fiscal support adds pressure to already strained supply chains, at least through mid-2021. In 2022, their contribution to the 1-year Treasury yield becomes negative as the expansionary effects of fiscal support wane.

Demand Shocks

Demand shocks initially contribute negatively to both output and prices, reflecting the collapse in private spending in 2020. At their peak contributions, demand shocks drag output down by about 5 percentage points in 2020 and prices down by 7 percentage points in mid-2021. From mid-2021 onward, a sequence of positive demand shocks boosts output, nearly offsetting their negative cumulative contribution to the price level, and supporting the lift-off in short-term interest rates starting in March 2022. Prior to that, demand shocks put downward pressure on interest rates. Demand shocks also contribute to higher delivery delays in 2021–2022 and add to the personal saving rate increases in 2020–2021, while they subtract thereafter.

Supply Chain Shocks

Supply chain shocks exert a persistent negative impact on output throughout the period under study. For prices, their influence becomes particularly important from 2021 onward, and by 2022, their cumulative effect is the dominant driver of the GDP deflator—reflecting widespread global bottlenecks and disruptions in logistics. Overall, supply chain shocks are the most important factor behind the rise in prices over the period analyzed. These shocks operate through delivery delays that translate into higher prices, particularly during 2020–2021. While their contributions to interest rates and the personal saving rate are positive in the early phase of the pandemic, their magnitudes are modest relatively to the contributions of the remaining shocks.

Cost-Push Shocks

Cost-push shocks constitute a dominant negative supply force in early 2020–2021, lowering output while pushing prices higher. Their relative contribution to prices is strongest in 2020, after which it diminishes as supply chain shocks take over. Cost-push shocks contribute negatively to delivery delays at the onset of the pandemic, but positively in 2021–2022, though the latter is less than the initial positive contribution of supply chain disruptions. We find a similar pattern in their contribution to unexpected movements in interest rates: negative for the period 2020–2021 and positive thereafter. Their effects on the personal saving rate are minor.

Monetary Policy Shocks

After a drop in interest rates in 2020:Q1, with short-term rates near the effective lower bound, inferred monetary policy shocks are predominantly contractionary between 2020:Q2 and late 2024, as policymakers face a limit on how much they can decrease rates to support the economy. These shocks add to the 1-year Treasury yield and, hence, contribute to a higher personal saving rate through higher interest rates. Because of this, they are a drag on output and prices from the start of the pandemic. While a sequence of accommodative shocks in late 2021 reduces their negative impact on output to roughly neutral, their contractionary influence on prices remains significant throughout the period. Our results therefore support the conclusion that monetary policy shocks are not responsible for the observed rise in prices during the period analyzed. In fact, in the absence of these shocks, the price level would be approximately 2 to 4 percentage points higher.

Summary

Taken together, the decomposition reveals a clear picture: fiscal transfer shocks support output through the end of 2021 but also put persistent upward pressure on the price level. Even so, they are not the dominant inflationary force. The bulk of the post-pandemic increase in the price level is driven primarily by supply shocks, which exert persistent upward pressure on prices while weighing on output. From late 2021 onward, demand shocks boost output and interest rates, but their cumulative contribution to the price level remains negative. Monetary

policy shocks help mitigate what might otherwise have been an even sharper rise in inflation.

4.1 Disentangling the Effects of Fiscal Transfers Shocks

Because the historical decomposition combines impulse responses with realized shocks, we disentangle these components to better understand the role of fiscal transfer shocks. We first present the inferred shocks and then examine their impulse responses.

Fiscal Transfer Shocks

Figure 5 depicts the posterior median and 68 percent posterior probability bands for the fiscal transfer shocks. The structural shocks recovered by our analysis are larger than typical shocks, with magnitudes as high as 50 under the unit-standard-deviation normalization. This indicates that the pandemic-related shocks lie far outside the range implied by pre-pandemic structural relations.

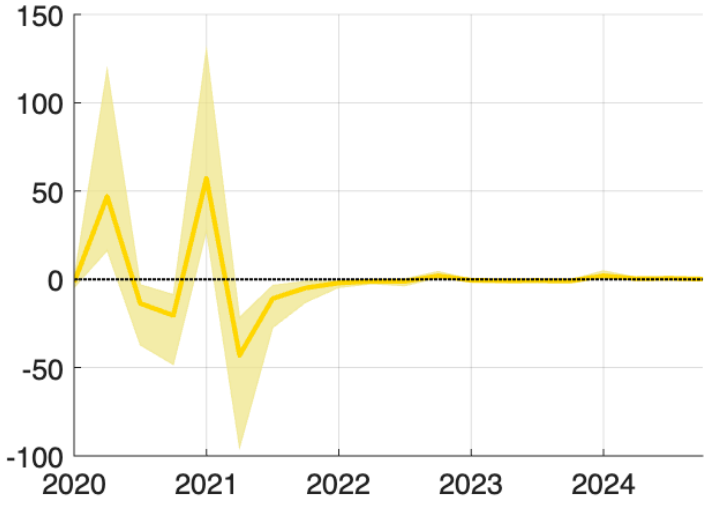

Figure 5: Fiscal Transfer Shocks. The solid curve represent the point-wise posterior median, and the shaded area represent the 68 percent equal-tailed point-wise probability bands.

The spike in 2020:Q2 corresponds to the CARES Act, and the spike in 2021:Q1 to the COVID-related Tax Relief Act of 2020 (enacted in late December 2020) and the American Rescue Plan. Each of these spikes is followed by large negative shocks, albeit of smaller

magnitude than the initial spike. This pattern partly reflects the persistence of the underlying structural relations: given the behavior of output and prices, the SVAR expects elevated transfers for longer. Looking beyond the COVID-related fiscal stimulus, fiscal transfer shocks hover around zero after 2022. Thus, fiscal transfer shocks are both positive and large, at least in 2020:Q2 and 2021:Q1. Next, we analyze the impulse responses to positive fiscal transfer shocks.

Impulse Responses

We focus on the impulse responses to a one-standard-deviation fiscal transfer shock, shown in Figure 6. As illustrated, a typical fiscal transfer shock leads to an increase of nearly 0.1 percentage point in the transfers-to-GDP ratio. This effect is persistent. Compared to the findings of Romer and Romer (2016), the persistence we observe in our identified fiscal transfer shocks is more aligned with their "permanent" shock scenario (lasting beyond 12 months) than with their "transitory" one (which fades after a month).

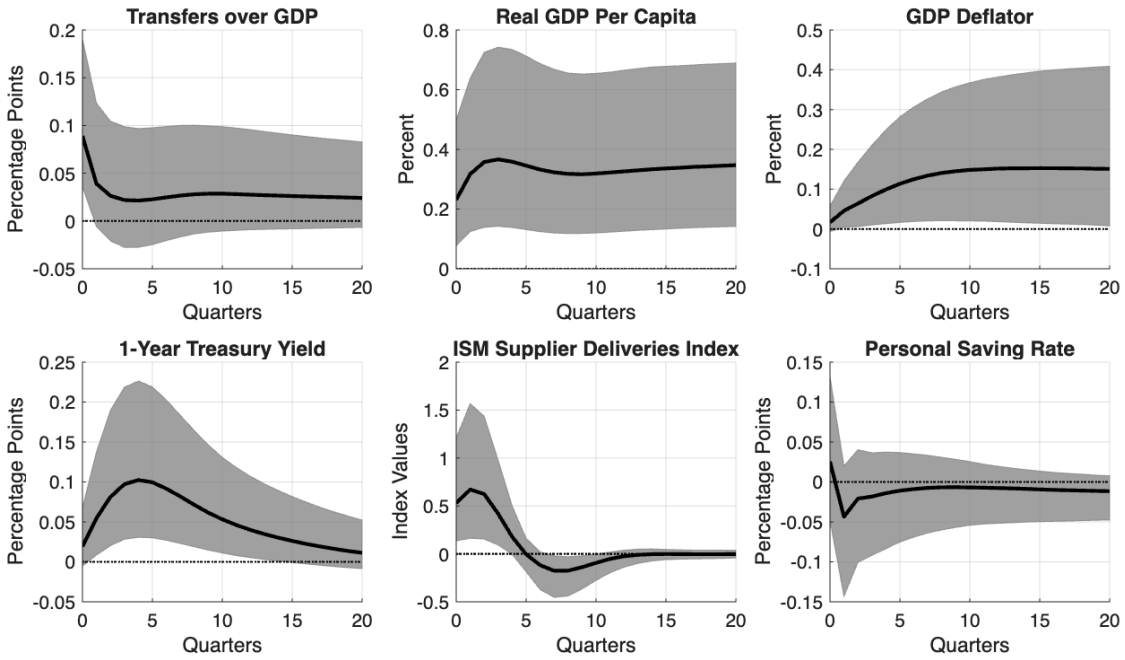

Figure 6: Impulse Responses to a Unit Standard Deviation Fiscal Transfer Shock

The response of the GDP deflator explains why this shock is inflationary. Despite the fact that the price level remains roughly unchanged on impact, the response builds gradually,

reaching a tad under 0.2 percent after five years. The effects of fiscal transfer shocks on output are more front-loaded. Real GDP increases by slightly more than 0.2 percent on impact and continues to rise, peaking at nearly 0.4 percent one year after the shock. Together, these two impulses explain the trade-off reported in the introduction to this section, as both prices and output rise after a fiscal transfer shock. Importantly, the response of output is broadly in line with the reaction of real consumption expenditures reported by Romer and Romer (2016) for their permanent transfer shock: their estimates suggest that a 1 percent increase in social benefits relative to personal income raises aggregate consumption by 1.2 percent in the month the bulk Social Security checks are received. Subsequently, consumption begins to decline. Since consumption constitutes a large share of output, we view their consumption response as broadly consistent with our response of output. These estimates also contribute to the ongoing debate on the effectiveness of fiscal transfers. Ramey (2025), for instance, questions their efficacy, arguing that the high marginal propensities to consume required to generate large effects either imply implausible macroeconomic counterfactuals or fail to account for macroeconomic endogeneity. Our findings provide a clear instance in which the standard empirical macroeconomic toolbox yields large positive effects of fiscal transfer shocks.

The large fiscal transfer shocks in 2020:Q2 and 2021:Q1 combined with these impulse responses explain both the immediate and substantial effects of fiscal transfer shocks on output, as well as the important and persistent but delayed effects on prices shown in Figure 4.

The 1-year Treasury yield also rises in response to the shock, in line with the positive short-term interest rate response to permanent transfers shocks reported by Romer and Romer (2016). Importantly, these effects are less persistent than the responses of output and prices. For this reason, the contribution of fiscal transfer shocks to the yield is less persistent than in the case of output and prices. Importantly, the systematic component of the monetary policy reaction to fiscal transfers may play a role offsetting both the expansionary and inflationary effects of fiscal transfer shocks.

The impulse response for the ISM Supplier Deliveries Index is overall similar to that of the 1-year Treasury yield. This explains why the contributions of fiscal transfer shocks to both the yield and the ISM Index show a broadly similar pattern. Finally, although the personal saving rate rises on impact and subsequently drops below zero, the wide probability

bands include zero, explaining the relatively minor contribution of the shock to this variable.

Together, the shape, magnitude, and co-movement of these impulse responses, along with the previously shown time series of shocks, provide key insights into three important results illustrated in Figure 4: (1) fiscal transfers have a sizable and persistent effect on prices, with the price level rising gradually but remaining elevated for a prolonged period, (2) output also benefits from fiscal transfers early on, though this contribution is less persistent than the effect on prices, and (3) monetary policy reacts to fiscal transfers, slightly dampening their expansionary and inflationary effects. This dampening is limited because the impact on yields is short-lived, peaking one year after the shock and then returning to baseline even as output and the price level stabilize at higher levels.

4.2 Comparison with Constant-Parameters SVAR

Since the time-varying approach used to obtain the results discussed above is computationally intensive, we ask what would have been different had we adopted a simpler constant-parameters SVAR. In order to answer that question, we compare our results with two alternative models. The first is a constant-parameters version of our time-varying model, using the same variables and same identification scheme; therefore, by comparing the results arising from the time-varying and constant parameters specifications in an otherwise identical setting we can isolate the role played by parameter variation. The second alternative model is the constant-parameters model of Giannone and Primiceri (2024). This second comparison is also interesting because, while they do not address fiscal transfer shocks, they analyze the role of demand and supply shocks behind the 2021–22 rise in inflation. Thus, the second comparison allows us to focus on the effects of considering transfers as an explanatory variable and identifying fiscal transfer shocks.

Constant-Parameters Version of Our Model

For the constant-parameters version of our model, we select a sample running from 1997 through 2019 and use the prior described in Section 3.4. Our sample choice aligns with Giannone and Primiceri (2024); Blanchard and Bernanke (2023) and tries to avoid the instabilities reported for the earlier periods. The identification strategy is the same as in the

time-varying model. The results for the constant-parameters model are shown in Figure 7. If

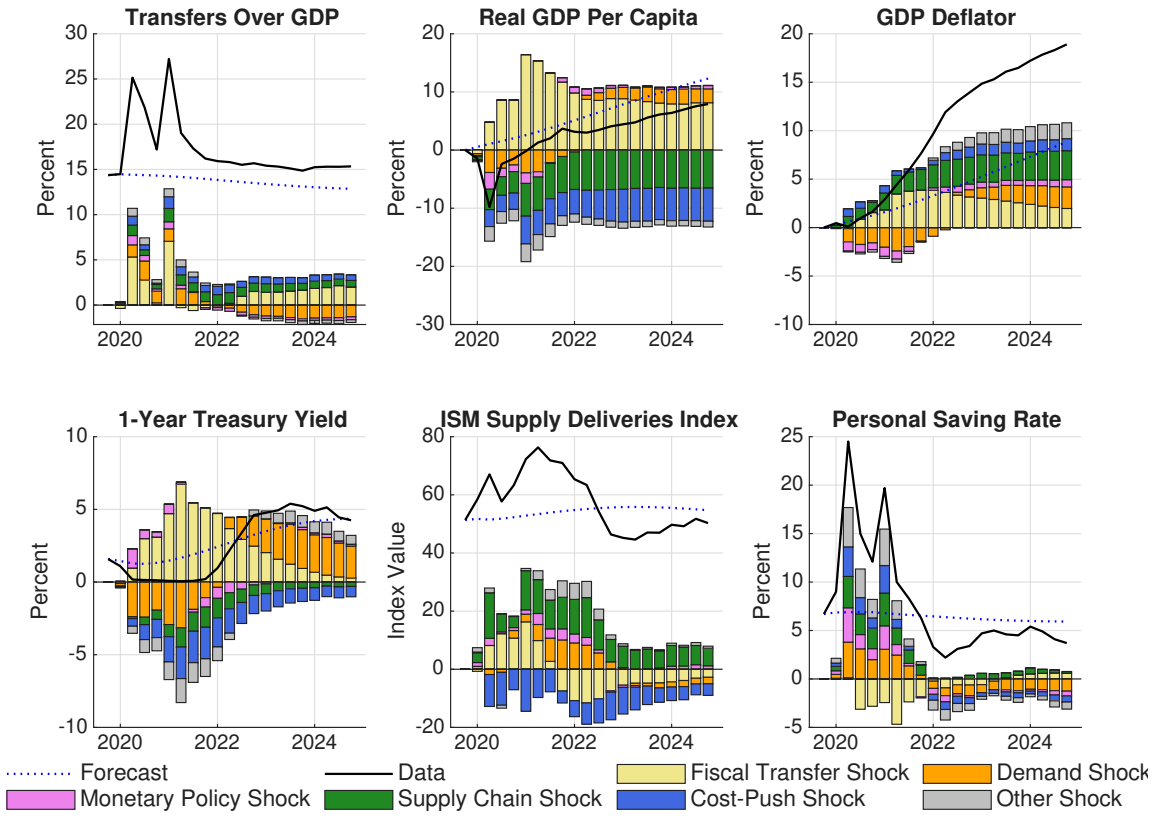

Figure 7: Constant-Parameters SVAR

we focus on the inflationary effects of fiscal transfer shocks, both the time-varying and the constant-parameters models deliver the same broad message: fiscal transfers are inflationary. Nevertheless, an important difference emerges: the positive effects of fiscal transfer shocks on output are considerably more persistent in the constant-parameters model. As a result, a researcher relying on the constant-parameters model would conclude that the output-inflation trade-off—supporting output in the short run at the cost of higher inflation in the long run—is more favorable to fiscal transfer shocks during downturns than suggested by the time-varying framework.

Importantly, while the time-varying model suggests that the contribution to the post-pandemic rise in the price level is mainly driven by supply-driven shocks (defined as the sum of cost-push and supply chain shocks) as demand-driven shocks (defined as the sum of demand, monetary, and fiscal transfer shocks) drag prices down, the constant parameter case suggests that both demand-driven and supply-driven shocks increase prices. Another

relevant difference emerging from this comparison is related to the role of monetary policy shocks. The time-varying model indicates that these shocks help contain prices, whereas the constant-parameters model suggests they are largely unimportant, even turning marginally inflationary toward the end of the period. Finally, the interpretation of demand drivers is different across the time-varying and the constant parameters models. The time-varying model shows that these shocks contribute strongly and positively to output, while their impact on prices is mostly negative. In contrast, the constant-parameters model suggests that demand drivers contribute strongly and positively to both output and prices during this period. Thus, a researcher relying on the constant-parameters model would conclude that demand-driver shocks are behind part of the unexpected post-pandemic increase in inflation, a conclusion that does not follow from the time-varying model.

In summary, the results differ in three key respects: (1) the output-stimulating effects of fiscal transfer shocks are larger in the constant parameter case, rendering the output–inflation trade-off emphasized in the time-varying approach less relevant; (2) demand-driven shocks emerge as a significant source of upward pressure to the price level in the constant parameter framework but they hold the price level down in the time-varying model; and (3) the latter difference is partly explained by the fact that the time-varying approach attributes a role to monetary shocks in containing price increases, whereas the constant parameters approach finds them to be largely irrelevant.

Comparison with Giannone and Primiceri (2024)

Giannone and Primiceri (2024) conduct several exercises, but their central analysis identifies one demand and one supply shock and study their contributions to the 2021–22 inflation. They conclude that "Post-COVID inflation was predominantly driven by unexpectedly strong demand forces [...] In comparison, the inflationary impact of adverse supply shocks was less pronounced, even though these shocks significantly constrained economic activity." To facilitate comparison with their results, Figure 8 aggregates our shocks into demand-driven shocks and supply-driven shocks.

As shown in the figure, our time-varying model yields a markedly different conclusion: post-COVID inflation is primarily driven by strong supply-driven shocks rather than demand-

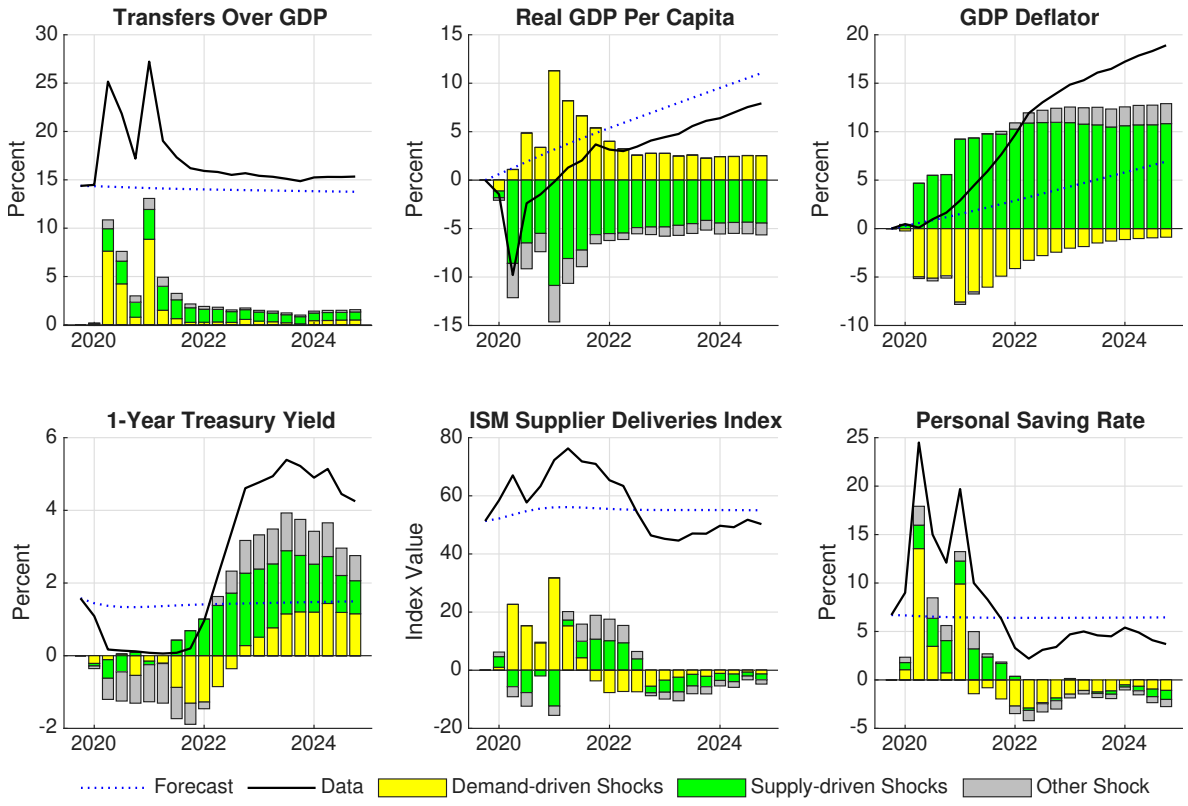

Figure 8: Time-Varying Parameters SVAR

driven shocks. In fact, in our model, demand-driven shocks push prices down. Both approaches agree that supply-driven shocks significantly constrain economic activity, but our time-varying specification further reveals that demand-driven shocks help sustain output in the early stages of the pandemic—whereas Giannone and Primiceri (2024) do not find this effect.

Conclusion After Comparison with Constant-Parameters SVAR

Thus, comparing our time-varying model with both the constant-parameters specification of our model and the results of the constant-parameters model of Giannone and Primiceri (2024) leads to two main conclusions. First, allowing for time variation in the parameters is essential to recognize that demand-driven shocks are not a major driver of inflation during this period; both constant-parameters models attribute a substantial inflationary role to demand-driven shocks while our time-varying model clarifies that the post-COVID surge in the price level is mostly a supply-driven shock phenomenon. Second, explicitly considering fiscal transfer shocks is crucial to uncover the supportive role of demand in sustaining output at the onset

of the pandemic. Both our constant-parameters and time-varying models considering fiscal transfer shocks conclude that demand-driven shocks supported output, while Giannone and Primiceri (2024), which does not consider these shocks, do not find this contribution.

5 The Shocks Behind the Great Recession

As highlighted in Section 2, transfers to persons as a share of GDP also rose during the Great Recession. We ask how much of this rise reflects exogenous fiscal transfer shocks rather than the systematic response of transfers to macroeconomic conditions. Our model confirms the common view that fiscal transfer shocks were smaller during the Great Recession than during the pandemic, with important implications for output and prices. Following the approach in Section 4, we re-estimate the model with the sample ending in 2007:Q4 and compute a historical decomposition starting in that quarter.

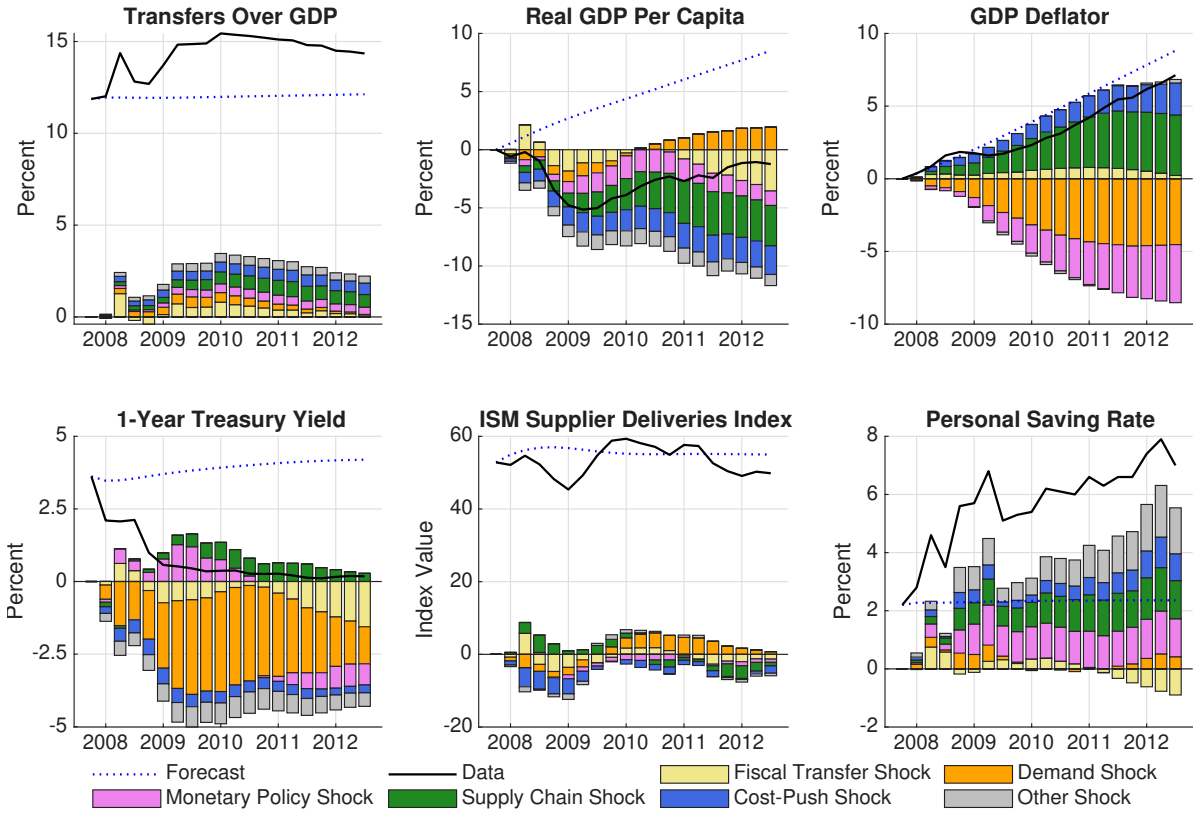

Figure 9: Great Recession

Figure 9 shows the posterior mean of the cumulative historical decomposition of the six

variables in our SVAR for 2008:Q1–2012:Q3. Before diving into the sources underlying the evolution of the U.S. economy during the Great Recession, let us highlight two features of the data that will serve as anchor points in our discussion. First, while inflation averaged about 3.5 percent annualized over the period 2020:Q1–2024:Q4, it was closer to 1.5 percent annualized during the Great Recession. Second, the growth rate of output per capita was about 1.8 percent annualized during the pandemic but it was negative during the Great Recession. We now analyze the shocks behind these differences.

Fiscal transfer shocks contribute little to the unexpected change in transfers-to-GDP—except in 2008:Q2, when most tax rebates from the Economic Stimulus Act of 2008 were disbursed (see, e.g., Shapiro and Slemrod, 2009). And, even in this quarter the absolute contribution to the unexpected increase in fiscal transfers was smaller than in the fiscal response to the pandemic. This supports the common view that exogenous transfer shocks during the Great Recession were smaller than during the pandemic. Instead, the increase in transfers-to-GDP largely reflects the systematic response of transfers to other shocks hitting the economy. Adverse supply chain and cost-push shocks push prices up, whereas negative demand shocks and contractionary monetary policy shocks push prices down. With fiscal transfer shocks small, their direct contribution to prices is negligible, helping explain why inflation was lower than during the pandemic. Output per capita receives little support from transfer shocks and falls by about 5 percent at its trough. Our time-varying SVAR attributes most of the unexpected output shortfall (around 10 percentage points relative to the 2007:Q4 forecast) to adverse supply shocks and contractionary monetary policy shocks. Overall, both demand-driven and supply-driven shocks depress output, but they move prices in opposite directions. Are small fiscal transfer shocks responsible for the different output and inflation outcomes relative to the pandemic? We address this question with a counterfactual exercise.

COVID-Sized Stimulus During the Great Recession

A key finding above is that fiscal transfer shocks during the Great Recession were much smaller than during the pandemic. Our estimates imply that pandemic-era transfer shocks were nearly four times larger and were central to both preventing an output collapse comparable

to the Great Depression and generating a much larger rise in the price level.[7] To isolate the role of shock size, we replay the Great Recession while replacing the estimated transfer shocks with the sequence identified for 2020–2024 (Figure 5).

Figure 10a presents the counterfactual evolution of output, prices, and yields along with their historical cumulative shock decomposition relative to the forecast as of 2007:Q4. The pandemic fiscal transfer shocks would have generated an early sizable increase in real GDP per capita, accompanied by a modest rise in prices. Importantly, both responses would have been smaller than those observed during the pandemic. This containment reflects a systematic monetary policy reaction that is stronger and faster in response to fiscal transfer shocks.

This counterfactual reinforces the main result discussed above: fiscal transfers can stabilize output, but at the cost of higher prices. It also underscores the critical role of monetary policy in shaping these outcomes. Specifically, the inflationary impact of fiscal transfer shocks depends on how aggressively the systematic component of monetary policy responds to them.

Figure 10b illustrates this latter point by comparing the contribution of fiscal transfer shocks to output, prices, and interest rates during the pandemic (maroon) and during the Great Recession in our counterfactual scenario (yellow bars), where we replace the Great Recession's fiscal shocks with those observed during the pandemic. The results are striking. Despite using the same sequence of fiscal shocks, the inflationary impact is notably smaller in the Great Recession scenario. This difference reflects the stronger and faster monetary policy response to fiscal shocks typical of that period.

This pattern is supported by Figure 11, which reports impulse responses to fiscal transfer shocks. The solid black lines show the median responses during the pandemic, while the red lines show the responses during the Great Recession under the counterfactual. The red lines demonstrate a larger and more front-loaded monetary reaction to fiscal transfer shocks as well as a persistent increase in the personal saving rate. In short, the same fiscal shocks generate smaller inflationary effects and more muted output gains when monetary policy responds more aggressively to them, as it did during the Great Recession. Importantly, the

[7] Fiscal transfer shock added about 5.3 percentage point to the increase in fiscal transfers over GDP in 2020:Q2, while they added 1.3 percentage point in 2008:Q2.

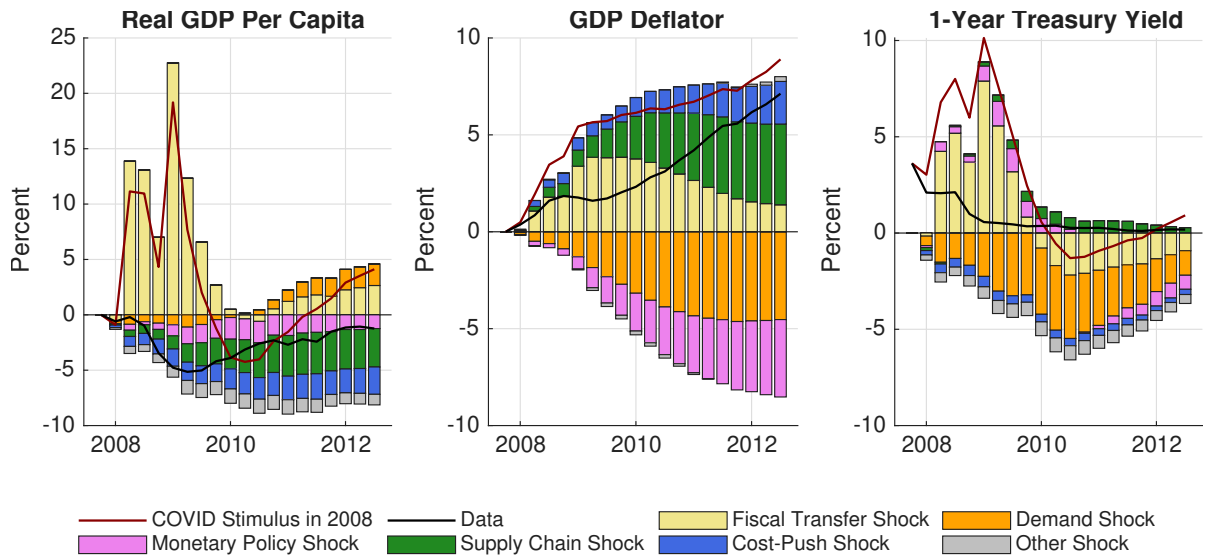

(a) Counterfactual Historical Shock Decomposition

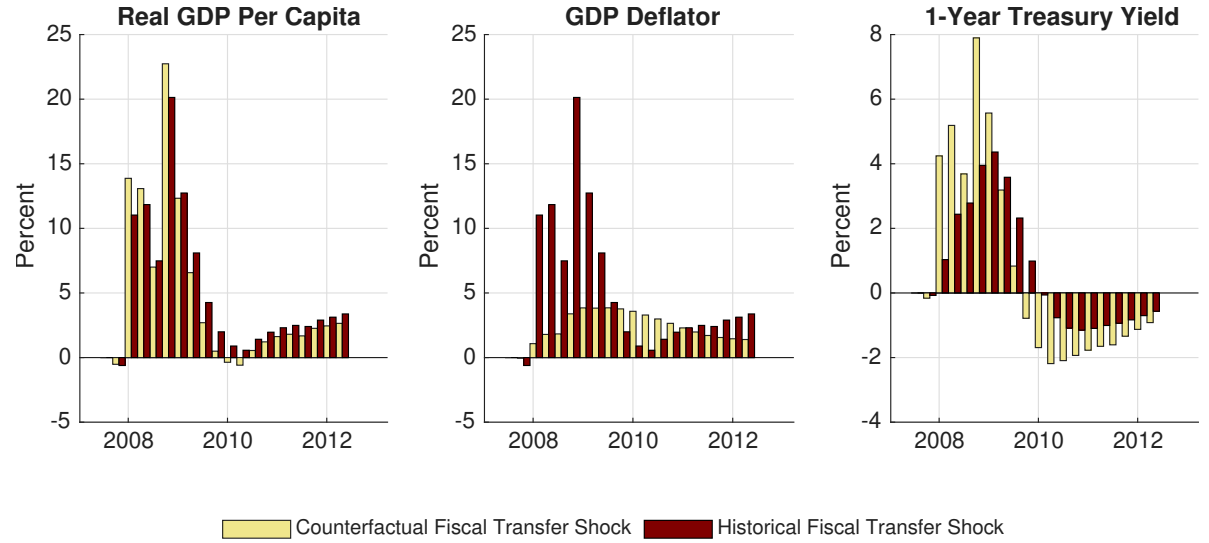

(b) Counterfactual vs Historical Fiscal Stimulus

Figure 10: COVID-Sized Stimulus during the Great Recession

personal saving rate also varies across episodes. During the pandemic, the short-run impulse response of the personal saving rate is negative, whereas it is positive in the counterfactual. This difference in sign may help explain the more moderate responses of both output and prices to fiscal transfer shocks.

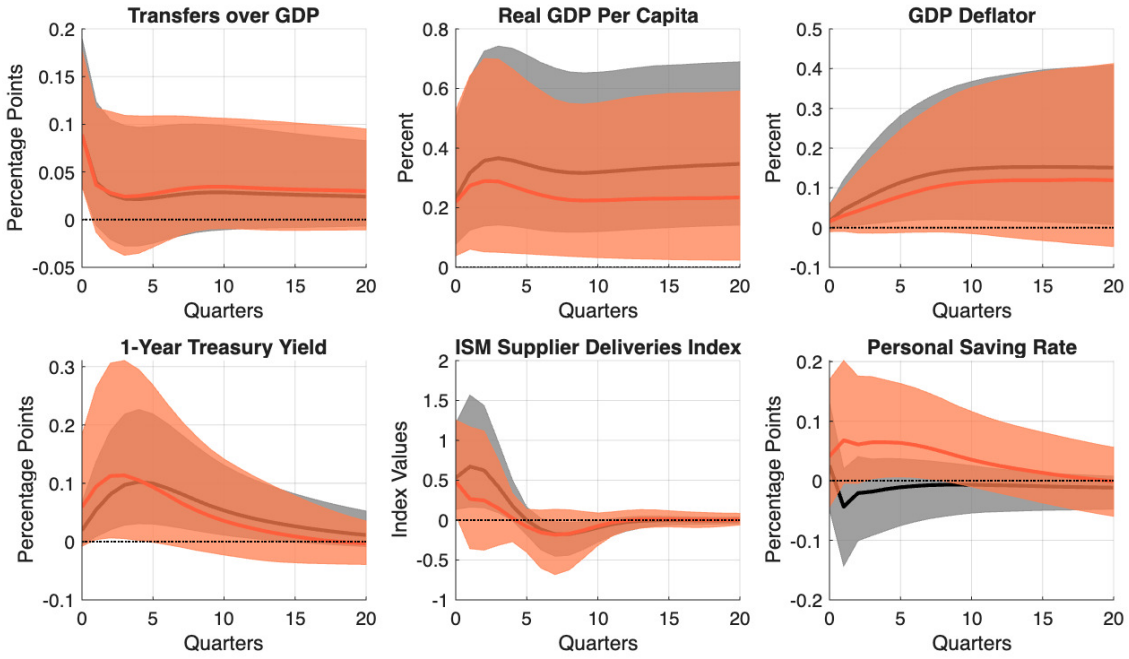

Figure 11: Impulse Responses Comparison. Solid black lines and gray-shaded areas correspond to the point-wise posterior median and 68 point-wise posterior probability bands for the impulse responses to a unit standard deviation shock in 2019:Q4. Solid red lines and red-shaded areas correspond to the point-wise posterior median and 68 point-wise posterior probability bands for the impulse responses to a unit standard deviation shock in 2007:Q4 scaled so that the median contemporaneous response to fiscal transfers is equal to the one from 2019:Q4.

Connection to Romer and Romer (2016)

This result confirms a conjecture in Romer and Romer (2016) that the effects of fiscal transfers on macroeconomic outcomes hinge on the response of monetary policy. Although they concentrated on real variables, not prices, our findings confirm their insight: the effectiveness of fiscal transfers is indeed shaped by how monetary policy reacts.[8] However, our results go a step further by showing that time dependence plays a critical role. Even when fiscal shocks are similar, their effects on output and inflation can differ substantially depending on when they occur, due to changes in the monetary reaction function over time or changes in the sensitivity of key margins of adjustment such as the personal saving rate.

[8] Romer and Romer highlight "One possible explanation for the seemingly short-lived response of consumption to a permanent benefit increase, and the contrast with the impact of a tax cut, involves the response of monetary policy[...]policy discussions reveal that policymakers were very aware of the benefit increases and often viewed them as a reason to tighten monetary policy."

The time-dependent impulse responses shown in Figure 11 further motivate the rotation-invariant time-varying SVAR framework used in this paper. Models that rely only on heteroskedasticity deliver time-invariant systematic monetary policy rules and time-invariant impulse responses, and therefore cannot capture the sharper, faster systematic monetary reaction to fiscal transfer shocks during the Great Recession.

6 Conclusion

We assess the inflationary effects of the U.S. fiscal response to the COVID-19 pandemic, leveraging advances in the identification of fiscal policy shocks in the recently proposed rotation-invariant time-varying SVAR. Our analysis suggests that fiscal transfer shocks account for a sizable share of the early post-pandemic increase in the price level through mid-2021. Thereafter, the rise in the price level is dominated by adverse supply shocks—especially supply-chain disruptions—while demand shocks mainly matter later for the lift-off in short-term interest rates. In addition, we find that fiscal transfers were essential for preventing a decline in real output per capita similar to the one experienced during the Great Depression. More broadly, we unveil an important role for monetary policy in shaping the trade-off between output stabilization and price stability. Muted monetary policy responses amplify the output effects of transfers but also increase their inflationary impact. In contrast, strong monetary policy responses can contain price pressures, albeit at the cost of weaker output support.

Appendix

I Prior over $\boldsymbol{\phi}$

Table I.1 summarizes the parameters and hyperparameters of the RC-SVAR. To facilitate the exposition, we partition $\boldsymbol{\phi}$ into fixed constant-parameters $\boldsymbol{\phi}_F$ and estimated constant-parameters $\boldsymbol{\phi}_E$, that is $\boldsymbol{\phi} = (\boldsymbol{\phi}_F, \boldsymbol{\phi}_E)$. The parameters in $\boldsymbol{\phi}_E$ depend on hyperparameters, which we denote by $\boldsymbol{\psi}$.

Table I.1: Model Parameters

Fixed Constant-Parameters: $\boldsymbol{\phi}_F$	
$\mathbf{m}_{\boldsymbol{\beta}_1}$	Expected value of $\boldsymbol{\beta}_1$.
$\mathbf{V}_{\boldsymbol{\beta}_1}$	Variance of $\boldsymbol{\beta}_1$.
$\boldsymbol{m}_{\boldsymbol{\delta}_1}$	Expected value of $\boldsymbol{\delta}_1$.
$\boldsymbol{V}_{\boldsymbol{\delta}_1}$	Variance of $\boldsymbol{\delta}_1$.
$\boldsymbol{m}_{\boldsymbol{\gamma}_1}$	Expected value of $\boldsymbol{\gamma}_1$.
$\boldsymbol{V}_{\boldsymbol{\gamma}_1}$	Variance of $\boldsymbol{\gamma}_1$.
Estimated Constant-Parameters: $\boldsymbol{\phi}_E$	
$\mathbf{V}_{\boldsymbol{\beta}}$	Variance of the innovations to $\boldsymbol{\beta}_t$.
$\mathbf{V}_{\boldsymbol{\delta}}$	Variance of the innovations to $\boldsymbol{\delta}_t$.
$\mathbf{V}_{\boldsymbol{\gamma}}$	Variance of the innovations to $\boldsymbol{\gamma}_t$.
Hyperparameters: $\boldsymbol{\psi}$	
$\bar{\nu}_{\boldsymbol{\beta}}$	Degrees of freedom of the prior for $\mathbf{V}_{\boldsymbol{\beta}}$.
$\bar{k}_{\boldsymbol{\beta}}$	Scaling factor for the scale matrix of the prior for $\mathbf{V}_{\boldsymbol{\beta}}$.
$\bar{\nu}_{\delta}$	Shape parameter of the prior for $V_{\delta,i}$ for $i = 1, \ldots, n$.
$\bar{k}_{\delta}$	Scaling factor for scale parameter of the prior for $V_{\delta,i}$ for $i = 1, \ldots, n$.
$\bar{\nu}_{\gamma}$	Shape parameter of the prior for $V_{\gamma,i}$ for $i = 1, \ldots, n_\gamma$.
$\bar{k}_{\gamma}$	Scaling factor for scale parameter of the prior for $V_{\gamma,i}$ for $i = 1, \ldots, n_\gamma$.

We assume a Dirac prior over $\boldsymbol{\phi}_F$; relaxing this assumption is possible at the cost of increased computation time. To set a value for $\boldsymbol{\phi}_F$, we follow Arias, Rubio-Ramirez, Shin, and Waggoner (2026) and base these parameters on the maximum likelihood estimate of a constant-parameters VAR with the same variables and lags as the time-varying specification. We estimate such a VAR using the first $T_0 = 60$ observations available in our sample. This number of observations represents about 25 percent of our sample; we view it as a conservative choice given the larger dimension of our TV-SVAR relative to existing studies. Accordingly, we set $\mathbf{m}_{\boldsymbol{\beta}_1}$ equal to the maximum likelihood estimate of a constant-parameters VAR which

we denote by $\hat{\mathbf{B}}$. We set $\mathbf{V}_{\boldsymbol{\beta}_1}$ equal to 4 times the unbiased estimator for the variance of $\hat{\mathbf{B}}$, as in Primiceri (2005). To set the values for $\boldsymbol{m}_{\boldsymbol{\delta}_1}$, $\boldsymbol{m}_{\boldsymbol{\gamma}_1}$, $\boldsymbol{V}_{\boldsymbol{\delta}_1}$ and $\boldsymbol{V}_{\boldsymbol{\gamma}_1}$, first it will be useful to let $\hat{\boldsymbol{\Sigma}}$ denote the maximum likelihood estimate of the variance of the reduced-form residuals of the constant-parameters VAR mentioned above, and second to define the following mapping between $\text{vech}(\hat{\boldsymbol{\Sigma}})$—where the vech operator stacks the elements on and below the main diagonal of a square matrix—and $(\boldsymbol{\delta}_1, \boldsymbol{\gamma}_1) : g\left(\text{vech}(\hat{\boldsymbol{\Sigma}})\right) = \left(\underbrace{2\log\left(\text{diag}(\hat{\mathbf{D}})\right)}_{\boldsymbol{\delta}_1}, \underbrace{\text{vecl}(\log \hat{\mathbf{C}})}_{\boldsymbol{\gamma}_1} \right)$, where $\hat{\mathbf{C}} = \hat{\mathbf{D}}^{-1}\hat{\boldsymbol{\Sigma}}\hat{\mathbf{D}}^{-1}$, $\hat{\mathbf{D}} = \left(\text{diag}(\text{diag}(\hat{\boldsymbol{\Sigma}}))\right)^{\frac{1}{2}}$, $\hat{\boldsymbol{\Sigma}} = (\text{vec}(\mathbf{I}_n)' \otimes \mathbf{I}_n)(\mathbf{I}_n \otimes (\mathbf{D}_n \, \text{vech}(\hat{\boldsymbol{\Sigma}})))$, and $\mathbf{D}_n$ is a $n^2 \times \frac{n(n+1)}{2}$ duplication matrix such that $\text{vec}(\hat{\boldsymbol{\Sigma}}) = \mathbf{D}_n \, \text{vech}(\hat{\boldsymbol{\Sigma}})$. By Proposition 3.4 of Lütkephol (2007),

$$\sqrt{T}\left(\text{vech}(\hat{\boldsymbol{\Sigma}}) - \text{vech}(\boldsymbol{\Sigma})\right) \to \text{N}(\mathbf{0}, 2\,\mathbf{D}_n^{+}(\boldsymbol{\Sigma} \otimes \boldsymbol{\Sigma})\,\mathbf{D}_n^{+\prime}),$$

where $\mathbf{D}_n^{+}$ is the Moore-Penrose generalized inverse of the duplication matrix $\mathbf{D}_n$. Then, by the Delta Method, $\sqrt{T}\left(g\left(\text{vech}(\hat{\boldsymbol{\Sigma}})\right) - g\left(\text{vech}(\boldsymbol{\Sigma})\right)\right) \to \text{N}(\mathbf{0}, \mathbf{D}_g(\boldsymbol{\Sigma}) 2\,\mathbf{D}_n^{+}(\boldsymbol{\Sigma} \otimes \boldsymbol{\Sigma})\,\mathbf{D}_n^{+\prime}\mathbf{D}_g(\boldsymbol{\Sigma})')$, where $\mathbf{D}_g(\boldsymbol{\Sigma}) = \frac{\partial g(\text{vech}(\boldsymbol{\Sigma}))}{\partial \text{vech}(\boldsymbol{\Sigma})}$. Let $\boldsymbol{V}_{g(\text{vech}(\hat{\boldsymbol{\Sigma}}))}(\boldsymbol{\Sigma}) = \frac{\mathbf{D}_g(\boldsymbol{\Sigma}) 2\,\mathbf{D}_n^{+}(\boldsymbol{\Sigma}\otimes\boldsymbol{\Sigma})\,\mathbf{D}_n^{+\prime}\mathbf{D}_g(\boldsymbol{\Sigma})'}{T}$. Thus, $\boldsymbol{m}_{\boldsymbol{\delta}_1} = 2\log\left(\text{diag}(\hat{\mathbf{D}})\right)$, $\boldsymbol{m}_{\boldsymbol{\gamma}_1} = \text{vecl}(\log \hat{\mathbf{C}})$

$$\boldsymbol{V}_{\boldsymbol{\delta}_1} = 4\begin{bmatrix} \mathbf{I}_n & \mathbf{0}_{n,n_\gamma} \end{bmatrix} \boldsymbol{V}_{g(\text{vech}(\hat{\boldsymbol{\Sigma}}))}(\hat{\boldsymbol{\Sigma}}) \begin{bmatrix} \mathbf{I}_n \\ \mathbf{0}_{n_\gamma,n} \end{bmatrix}, \text{ and } \quad \boldsymbol{V}_{\boldsymbol{\gamma}_1} = 4\begin{bmatrix} \mathbf{0}_{n_\gamma,n} & \mathbf{I}_{n_\gamma} \end{bmatrix} \boldsymbol{V}_{g(\text{vech}(\hat{\boldsymbol{\Sigma}}))}(\hat{\boldsymbol{\Sigma}}) \begin{bmatrix} \mathbf{I}_{n_\gamma} \\ \mathbf{0}_{n,n_\gamma} \end{bmatrix},$$

where $\mathbf{I}_s$ is the identity matrix of dimension $s \times s$ and $\mathbf{0}_{s_1,s_2}$ is a matrix of zeros of dimension $s_1 \times s_2$. The prior over $\boldsymbol{\phi}_E$, i.e., $p(\boldsymbol{\phi}_E \mid \boldsymbol{\phi}_F, \boldsymbol{\psi})$, is as follows: $\mathbf{V}_{\boldsymbol{\beta}} \sim \text{IW}(\bar{\nu}_{\boldsymbol{\beta}} \bar{k}_{\boldsymbol{\beta}}^2 \boldsymbol{V}_{\boldsymbol{\beta}_1}, \bar{\nu}_{\boldsymbol{\beta}})$, $V_{\delta,i} \sim \text{IG}\left(\frac{\bar{\nu}_\delta}{2}, \frac{\bar{\nu}_\delta \bar{k}_\delta^2 (e_{i,n}' \boldsymbol{V}_{\boldsymbol{\delta}_1} e_{i,n})}{2}\right)$ for $i = 1, \ldots, n$, and $V_{\gamma,i} \sim \text{IG}\left(\frac{\bar{\nu}_\gamma}{2}, \frac{\bar{\nu}_\gamma \bar{k}_\gamma^2 (e_{i,n_\gamma}' \boldsymbol{V}_{\boldsymbol{\gamma}_1} e_{i,n_\gamma})}{2}\right)$ for $i = 1, \ldots, n_\gamma$ where $e_{i,x}$ denotes the i-th column of an identity matrix of dimension x. The scale parameters are chosen to be constant fractions of the maximum likelihood estimated variances of the corresponding subsample. In particular, $\bar{k}_{\boldsymbol{\beta}} = 0.01$ and $\bar{k}_\delta = \bar{k}_\gamma = 0.1$. We choose the fractions to be larger for $V_{\delta,i}$ and $V_{\gamma,i}$. This choice reflects our prior belief that most of the time variation is on the variance of the reduced-form innovations (see, for example Sims and Zha, 2006). The shape parameters are chosen to be the smallest natural number such that the densities are defined. The degrees of freedom, $\bar{\nu}_{\boldsymbol{\beta}}$, are set equal to 105, which is moderately larger than the minimum possible number of degrees of freedom for which the density is defined. As in Primiceri (2005), this choice seems to be necessary in order to avoid

implausible behavior of the time-varying slope coefficients. Overall, the priors are as diffuse and uninformative as possible (see Primiceri, 2005, for a similar motivation).

II Disentangling the Historical Decomposition

In this appendix, we discuss the role of other shocks in the historical decomposition described in Section 4.1. The impulse responses to a unit standard deviation demand shock are shown in Figure II.1. By assumption, real GDP, the GDP deflator, and the 1-year Treasury yield increase upon impact in response to this shock. These increases persist for more than a year according to the posterior medians. As real GDP increases, the transfers-to-GDP ratio declines persistently. Consistent with the higher demand for output, the ISM Supplier Deliveries Index also increases in the near term even though this effect is less precisely estimated. The response of the personal saving rate is imprecisely estimated.

Next, we report impulse responses to a unit standard deviation monetary policy shock (Figure II.2). We identify this shock by assuming that output and inflation decrease, while the 1-year Treasury yield increases, upon impact. As in the case of the demand shock, the monetary policy shock has persistent effects on real GDP, the GDP deflator, and the 1-year Treasury yield. Transfers and the personal saving rate move in the expected direction as economic conditions deteriorate and the real interest rate increases. The ISM Supplier Deliveries Index also increases.

Moving on to the impulse responses to the supply chain and cost-push shocks. Figure II.3 shows the responses to a supply chain shock and Figure II.4 shows the responses to a cost-push shock. Recall that these shocks are identified with identical assumptions except for the impact response on the ISM Supplier Deliveries Index. This deconstruction of supply shocks offers valuable insights. First, the response of the GDP deflator to a supply chain shock is noticeably larger than the response to a cost-push shock. The price level increases by about 0.07 percent upon impact in response to a unit standard deviation supply chain shock. This response builds up, peaking at about 0.4 percent five years after the shock. The price level also increases by 0.07 percent upon impact in response to a unit standard deviation cost-push shock and builds up thereafter, although it peaks at a lower value than in the case

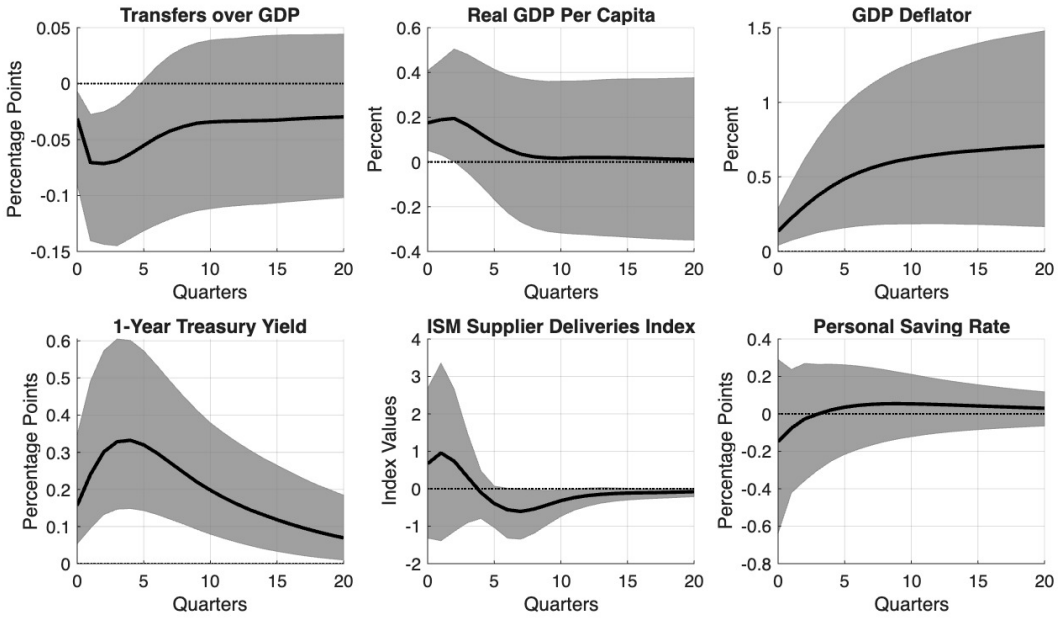

Figure II.1: Impulse Responses to a Unit Standard Deviation Demand Shock

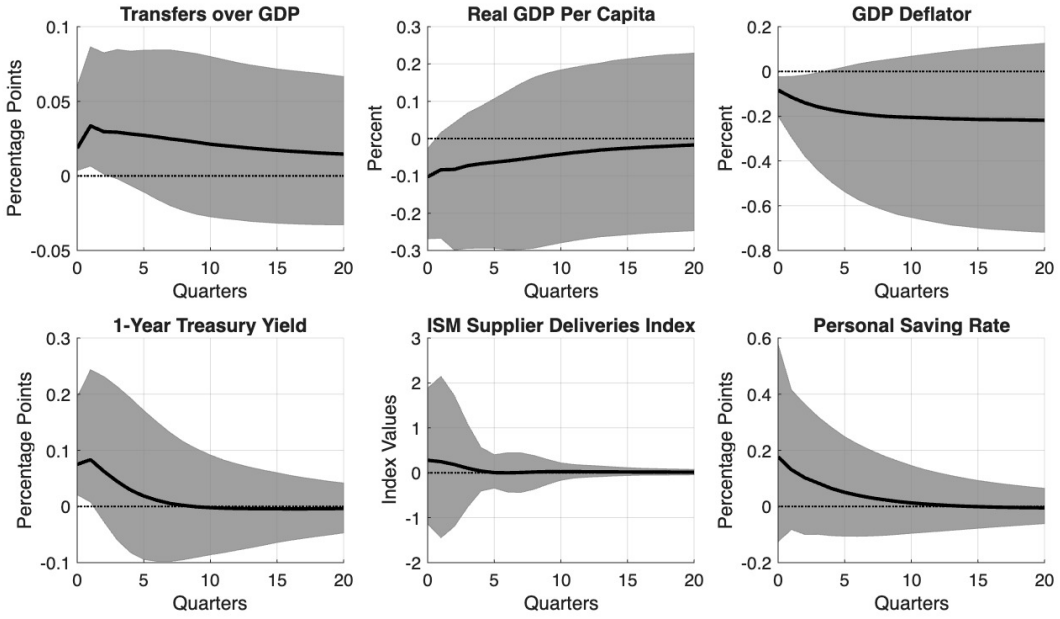

Figure II.2: Impulse Responses to a Unit Standard Deviation Monetary Shock

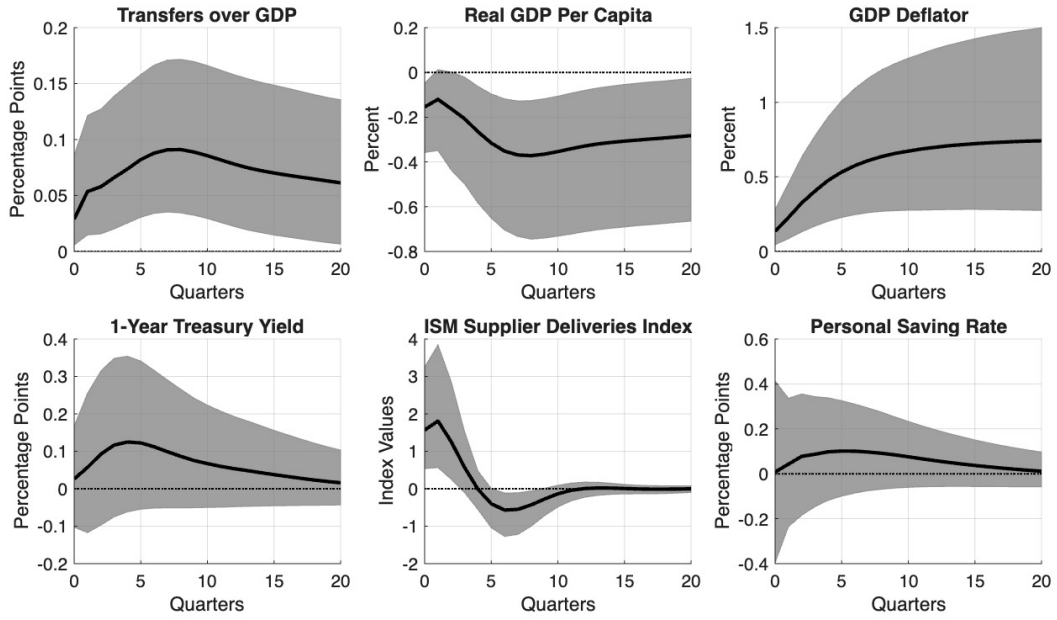

Figure II.3: Impulse Responses to a Unit Standard Deviation Supply Chain Shock

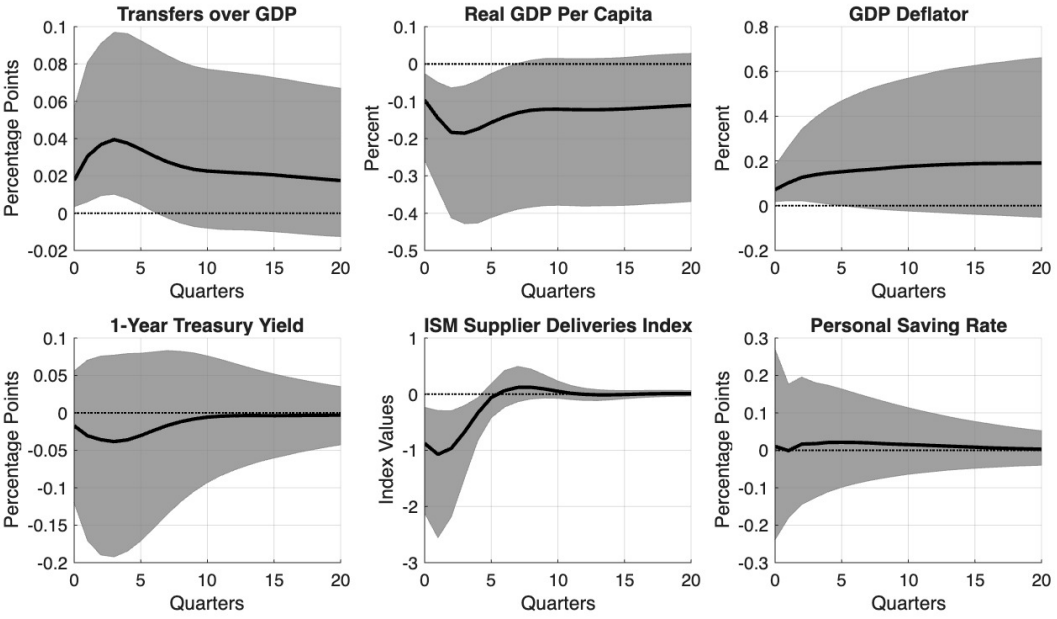

Figure II.4: Impulse Responses to a Unit Standard Deviation Cost-Push Shock

of supply chain shocks, 0.15 percent. Turning to output, the decline in real GDP upon impact is less pronounced in the case of a supply chain shock relative to the decline in response to a cost-push shock. However, the decline in real GDP is larger and more persistent in the case of supply chain shocks: the trough response of real GDP to supply chain shocks is about -0.3 percent after two years, while it is -0.25 percent after one year in the case of cost-push shocks. The different responses of the price level and output are consistent with the different responses of the 1-year Treasury yield: while it increases in response to a supply chain shock, it decreases in response to a cost-push shock. Accordingly, monetary policy fights the rise in inflation more aggressively in response to supply chain shocks. The response of transfers is positive in both cases as economic conditions deteriorate, with a more front-loaded response to a cost-push shock in line with the patterns of the impulse responses of real GDP. The response of the personal saving rate is imprecisely estimated in both cases.

Figure II.5 describes the time-series of the implied structural shocks.

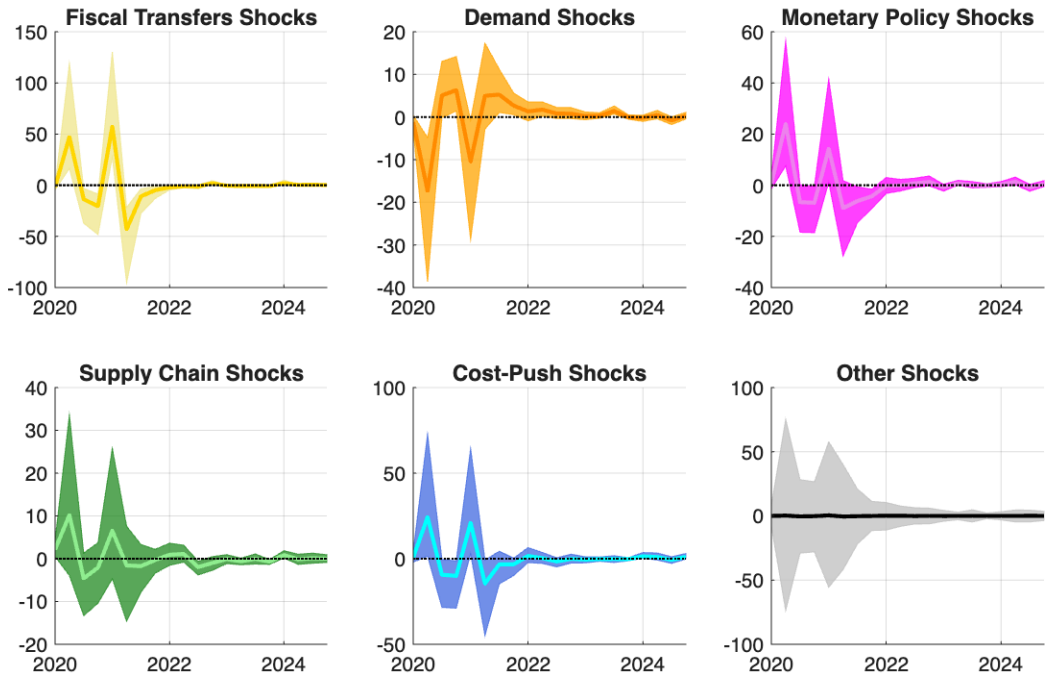

Figure II.5: Structural Shocks

Finally, Table II.1 shows the systematic component of fiscal transfer policy implied by our identification scheme. As it can be seen, the posterior median implied by our model is

nearly identical to the negative elasticity of unemployment-related expenditure to output estimated by Giorno, Richardson, Roseveare, and van den Noord (1995) for the U.S. The 68 percent probability bands suggest that the probability mass is not concentrated near the upper bound imposed by our identification scheme.

Coefficient	ψ_y	ψ_p	ψ_i	ψ_d	ψ_{psr}
Median	-0.20	0	0	0	0
68% Prob. Interval	[-0.55;-0.05]	[0;0]	[0;0]	[0;0]	[0;0]

Table II.1: Fiscal Transfers Equation

NOTE: The entries in the table denote the posterior median estimates of the contemporaneous coefficients in the fiscal transfers equation under our identification. The 68 percent equal-tailed posterior probability intervals are reported in brackets.

III Probability Bands for Historical Decomposition

In this appendix, we supplement Figure 4 by reporting 68 percent point-wise probability bands around the posterior means. For ease of visualization, we plot the contribution of each shock in a separate figure (Figures III.1-III.5). The probability bands support the qualitative conclusions based on posterior means. For example, the probability bands for the contribution of fiscal transfer shocks to output and the price level are mostly positive. Demand shocks emerge as important negative contributors to output and the price level. Monetary policy shocks are contractionary at the onset of the pandemic and therefore contribute negatively to output and the price level. Supply chain shocks are the single most important contributor to the price level. Cost-push shocks contribute negatively to output and positively to the price level during 2020 and 2021.

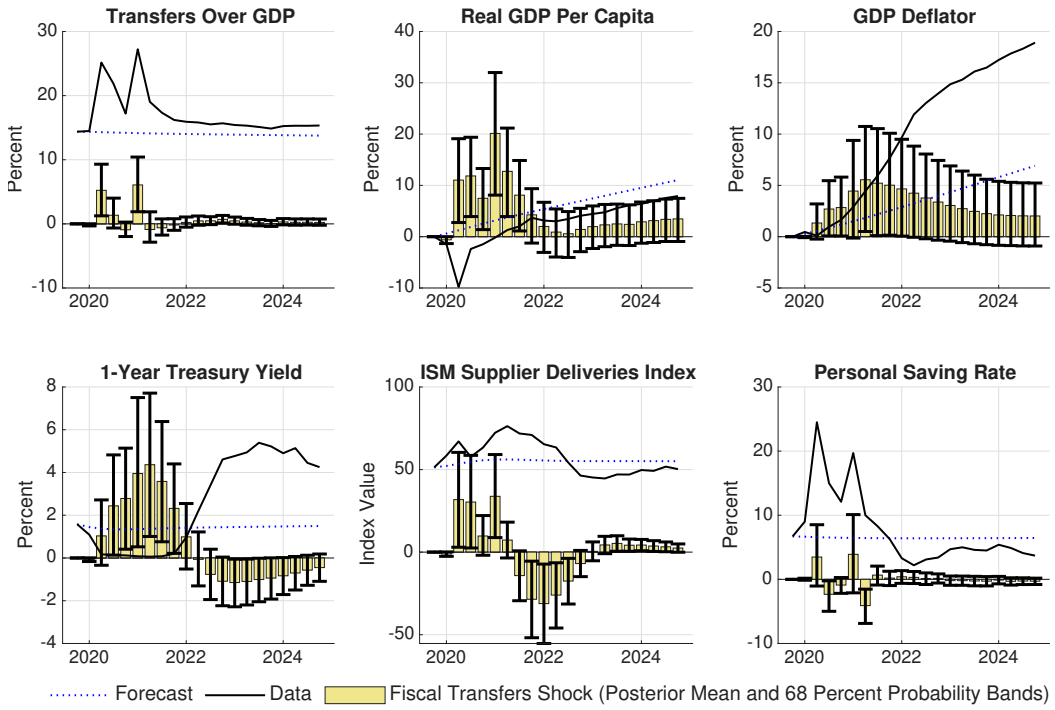

Figure III.1: Fiscal Transfer Shock Contribution: Posterior Mean and 68% Bands

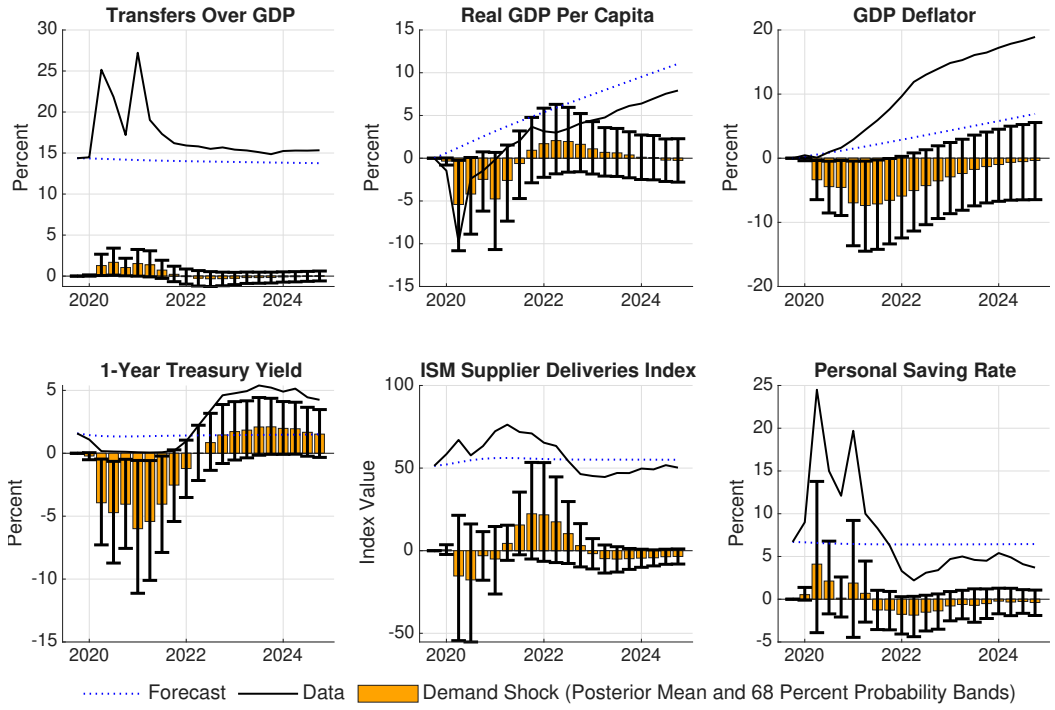

Figure III.2: Demand Shock Contribution: Posterior Mean and 68% Bands

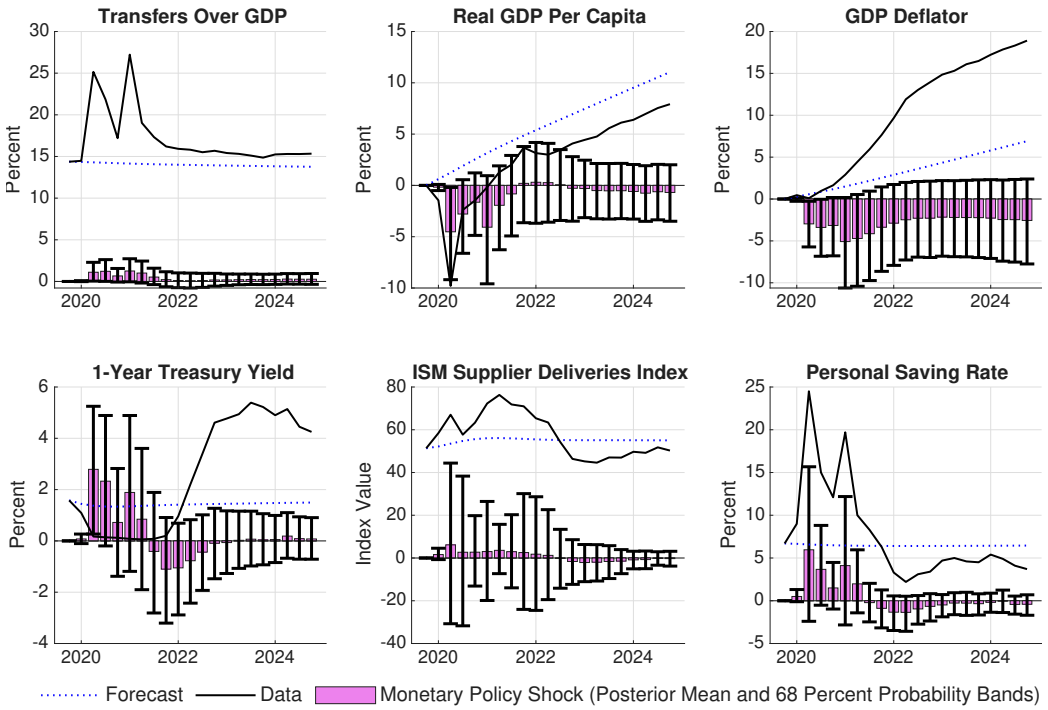

Figure III.3: Monetary Policy Shock Contribution: Posterior Mean and 68% Bands

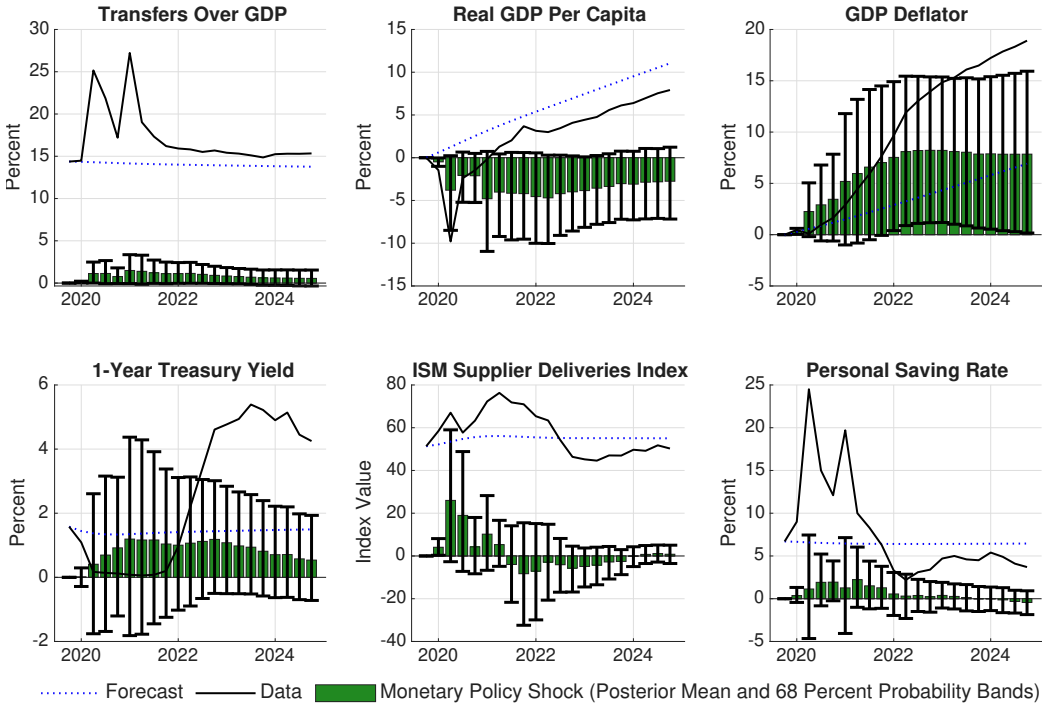

Figure III.4: Supply Chain Shock Contribution: Posterior Mean and 68% Bands

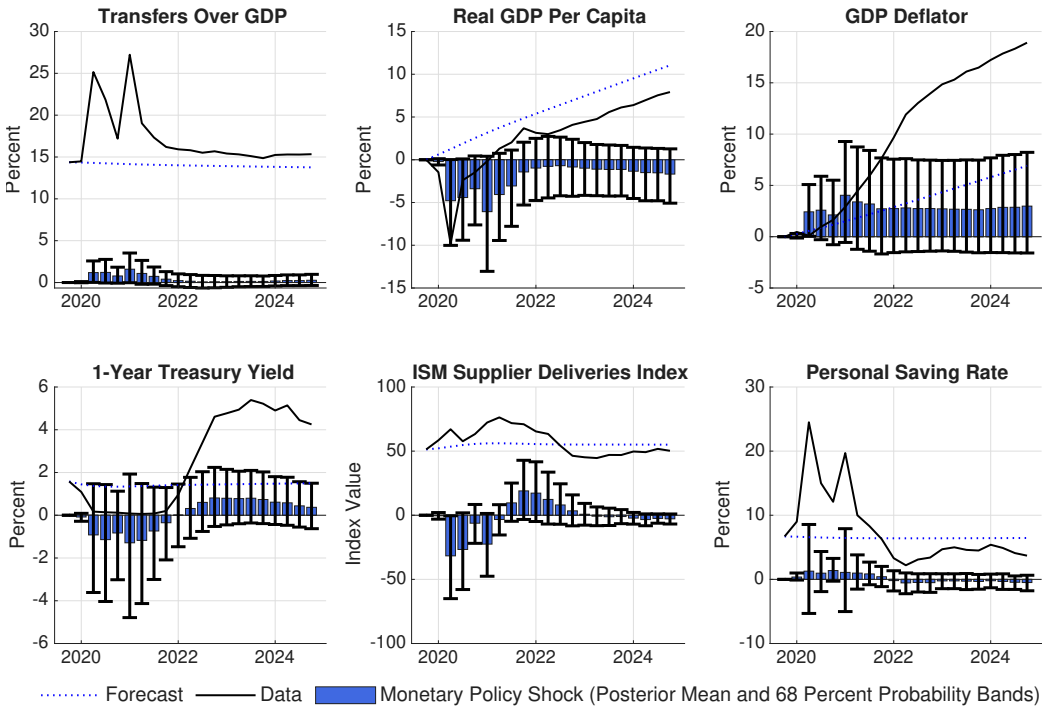

Figure III.5: Cost-Push Shock Contribution: Posterior Mean and 68% Bands

IV Convergence

In this section, we evaluate the convergence of the Gibbs Sampler algorithm. We focus our analysis on three well-known measures to judge the sampling properties of the algorithm: the auto-correlation function, the inefficiency factors (that is, the inverse of the relative numerical efficiency measure of Geweke, 1992), and the diagnostic proposed by Raftery and Lewis (1992) for the total number of draws that are necessary to achieve a given precision.

The model features a large number of time-varying parameters. Since we identify the first five equations in the RC-SVAR, when reporting convergence diagnostics for $(\mathbf{A}_t, \mathbf{F}_t)_{t=1}^T$ we focus on the corresponding blocks and denote them by $(\mathbf{A}_{\cdot 1:5,t})_{t=1}^T$ and $(\mathbf{F}_{\cdot 1:5,t})_{t=1}^T$, respectively. We also report diagnostics for the hyperparameters $\mathbf{V}_{\boldsymbol{\delta}}$, $\mathbf{V}_{\boldsymbol{\gamma}}$, and $\mathbf{V}_{\boldsymbol{\beta}}$ governing time variation.

Following Primiceri (2005), we report the 20th-order sample auto-correlation. Figure IV.1 shows the results for the time-varying structural parameters in $(\mathbf{A}_{\cdot 1:5,t}, \mathbf{F}_{\cdot 1:5,t})_{t=1}^T$ and for selected hyperparameters. As can be seen, the auto-correlation of the structural parameters is below 0.5 for most parameters and below 0.25 for nearly all structural parameters. Turning to the hyperparameters $(V_{\delta_i})_{i=1}^n$ and $(V_{\gamma_i})_{i=1}^{n_\gamma}$, the 20th-order auto-correlation is below or about

0.25 in most cases. The hyperparameters $\mathbf{V}_{\boldsymbol{\beta}}$ exhibit somewhat more correlation, but we conduct several runs with different seeds and find the results robust to this feature.

Next, we discuss the inefficiency factors defined as $(1 + 2\sum_{k=1}^{\infty} \rho_k)$. These factors are inversely related to the relative numerical efficiency measure of Geweke (1992). In particular, $(1 + 2\sum_{k=1}^{\infty} \rho_k) = \frac{2\pi S_G(0)}{\gamma_0}$ where $S_G(0)$ denotes the spectral density evaluated at frequency zero and γ_0 denotes the variance of the draws. It estimates the approximate number of correlated draws (from our Gibbs Sampler) required to match the variance in the posterior sample mean that would be obtained from uncorrelated draws (ideal but infeasible). We compute $S_G(0)$ using Bartlett's weights. Figure IV.2 plots the results and Table IV.1 provides a summary. Overall, the inefficiency factors for the structural parameters are around or below 20, which is a number typically considered satisfactory. As in the case of the auto-correlation, the hyper-parameters have higher inefficiency factors.

To conclude, following Raftery and Lewis (1992) we estimate the number of draws required to achieve a given precision when estimating posterior moments of the parameters. We use the implementation of these statistics in the Econometrics Toolbox, developed by James P. LeSage; we set the desired quantile equal to 0.025, the desired accuracy to 0.025, and the probability of covering the desired accuracy to 0.95. Figure IV.3 shows the results. For all of the parameters, the required number of draws is below the number of draws used in our analysis.

	Median	Mean	Min	Max	10-th Percentile	90-th Percentile
$(\mathbf{A}_{\cdot 1,t})_t^T$	0.99	1.01	0.56	7.25	0.87	1.13
$(\mathbf{F}_{\cdot 1,t})_t^T$	0.99	1.03	0.34	37.88	0.86	1.13
$\mathbf{V}_{\boldsymbol{\delta}}$	13.25	14.39	10.13	22.81	10.22	22.12
$\mathbf{V}_{\boldsymbol{\gamma}}$	25.38	26.36	17.15	39.10	19.73	36.02
$\mathbf{V}_{\boldsymbol{\beta}}$	19.88	25.77	4.35	90.22	8.87	53.46

Table IV.1: Summary of Inefficiency Factors

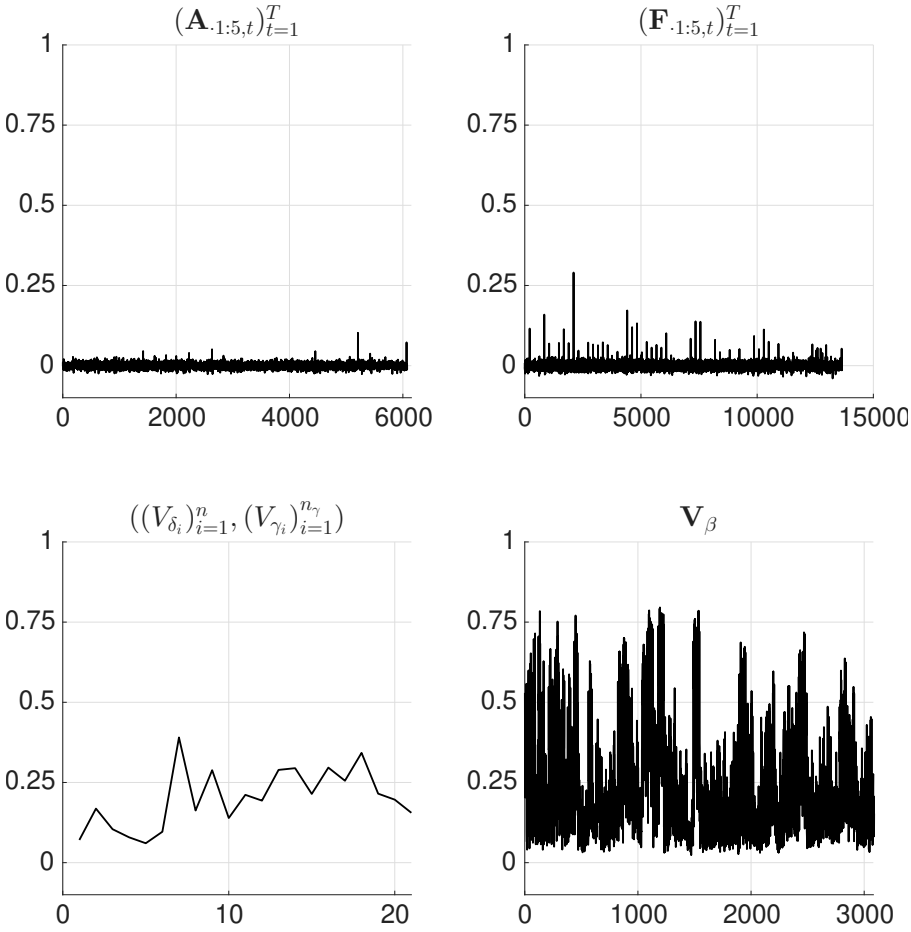

Figure IV.1: 20th-Order Sample Auto-Correlations

Note: The upper panels report 20th-order sample auto-correlations for the time-varying structural parameters in the identified block, $(\mathbf{A}_{\cdot 1:5,t})_{t=1}^{T}$ and $(\mathbf{F}_{\cdot 1:5,t})_{t=1}^{T}$. The bottom panels report the corresponding auto-correlations for selected hyperparameters governing time variation.

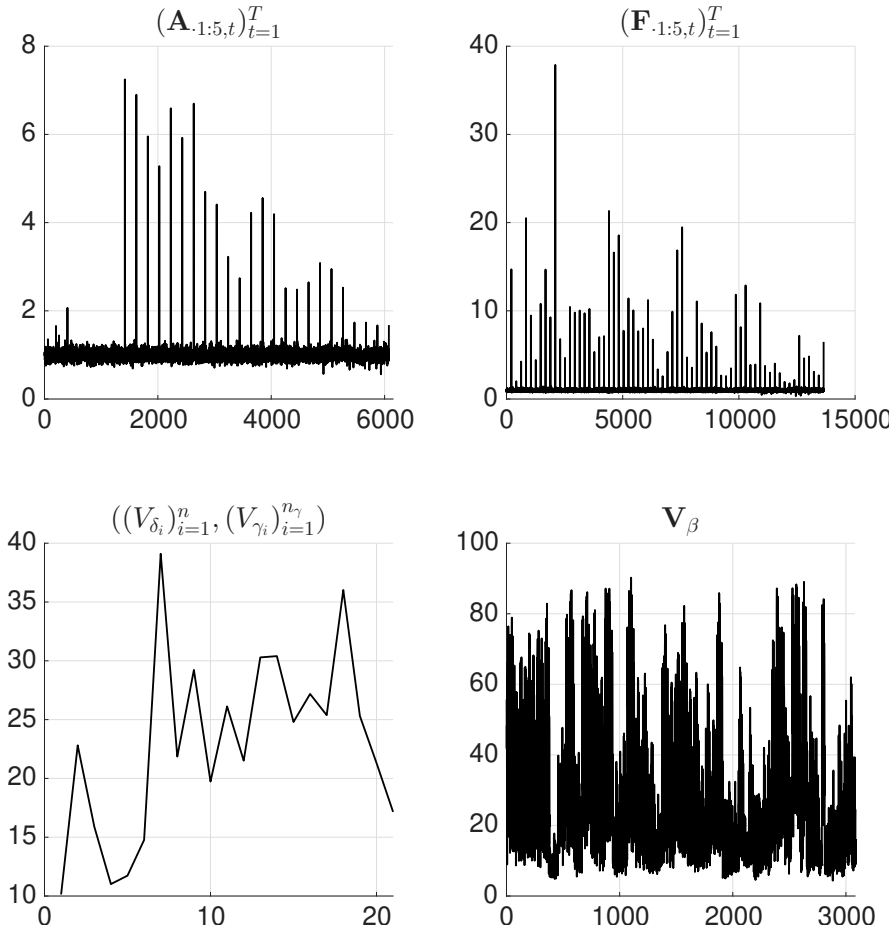

Figure IV.2: Inefficiency Factors

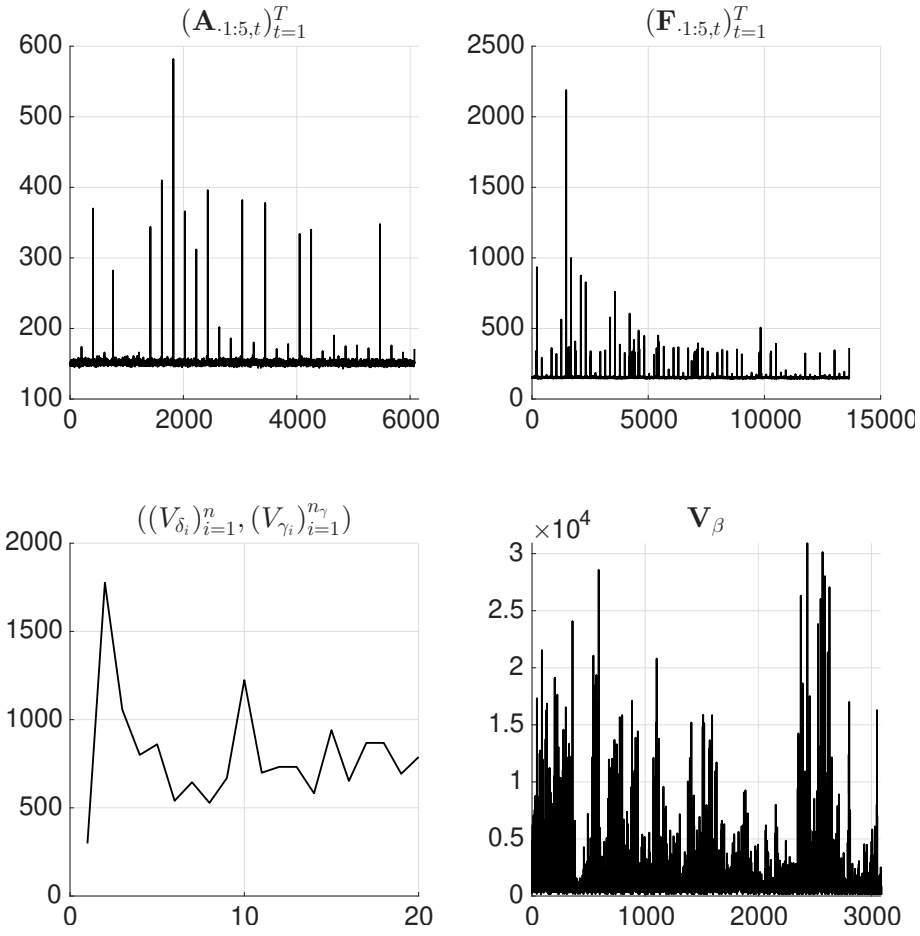

Figure IV.3: Number of Draws for Given Precision

References

Akinci, O., G. Benigno, R. Heymann, J. di Giovanni, J. Groen, L. Lin, and A. Noble (January 28 2022). The Global Supply Side of Inflationary Pressures. Technical report, Federal Reserve Bank of New York.

Angeletos, G.-M., C. Lian, and C. K. Wolf (2024). Can deficits finance themselves? *Econometrica 92*(5), 1351–1390.

Archakov, I. and P. R. Hansen (2021). A New Parametrization of Correlation Matrices. *Econometrica 89*(4), 1699–1715.

Arias, J. E., J. F. Rubio-Ramirez, and M. Shin (2025). Large SVARs. Working Paper 26-04, Federal Reserve Bank of Philadelphia.

Arias, J. E., J. F. Rubio-Ramirez, M. Shin, and D. F. Waggoner (2026). Inference Based on Time-varying SVARs Identified with Sign Restrictions. *Review of Economic Studies (forthcoming)*.

Arias, J. E., J. F. Rubio-Ramírez, and D. F. Waggoner (2018). Inference Based on Structural Vector Autoregressions Identified with Sign and Zero Restrictions: Theory and Applications. *Econometrica 86*(2), 685–720.

Ascari, G., D. Bonam, L. Mori, and A. Smadu (2024). Fiscal policy and inflation in the euro area. Working Paper 820, De Nederlandsche Bank.

Bai, X., J. Fernandez-Villaverde, Y. Li, and F. Zanetti (2024). The causal effects of global supply chain disruptions on macroeconomic outcomes: Evidence and theory. Working Paper 32098, National Bureau of Economic Research.

Benigno, G., J. di Giovanni, J. J. J. Groen, and A. I. Noble (2022). The GSCPI: A New Barometer of Global Supply Chain Pressures. Staff Report 1017, Federal Reserve Bank of New York.

Bergholt, D., F. Canova, F. Furlanetto, N. Maffei-Faccioli, P. Ulvedal, et al. (2024). What Drives the Recent Surge in Inflation? The Historical Decomposition Rollercoaster. Technical report, CEPR Discussion Papers.

Bianchi, F., R. Faccini, and L. Melosi (2023). A Fiscal Theory of Persistent Inflation. *Quarterly Journal of Economics 138*(4), 2127–2179.

Blanchard, O. and B. S. Bernanke (2023). What Caused the US Pandemic-Era Inflation? Working Paper 31417, National Bureau of Economic Research.

Blanchard, O. and R. Perotti (2002). An Empirical Characterization of the Dynamic Effects of Changes in Government Spending and Taxes on Output. *The Quarterly Journal of Economics 117*(4), 1329–1368.

Bognanni, M. (2018). A Class of Time-Varying Parameter Structural VARs for Inference under Exact or Set Identification. *Federal Reserve Bank of Cleveland Working Paper 1*(18-11), 1–61.

Brunnermeier, M., D. Palia, K. Sastry, and C. Sims (2021). Feedbacks: Financial markets and economic activity. *American Economic Review 111*, 1845–1879.

Caldara, D. and C. Kamps (2017). The Analytics of SVARs: A Unified Framework to Measure Fiscal Multipliers. *Review of Economic Studies 84*(3), 1015–1040.

Cochrane, J. H. (2022). Inflation and the end of illusions. Blog post, The Grumpy Economist.

di Giovanni, J. (2022). How Much Did Supply Constraints Boost U.S. Inflation? Liberty Street Economics (Federal Reserve Bank of New York).

di Giovanni, J., c. Kalemli-́Ozcan, A. Silva, and M. A. Yildirim (2022). Global Supply Chain Pressures, International Trade, and Inflation. Working Paper 30240, National Bureau of Economic Research.

Gertler, M. and P. Karadi (2015). Monetary Policy Surprises, Credit Costs, and Economic Activity. *American Economic Journal: Macroeconomics 7*(1), 44–76.

Geweke, J. (1992). Evaluating the Accuracy of Sampling-Based Approaches to the Calculation of Posterior Moments. In J. Bernardo, J. Berger, A. P. Dawid, and A. Smith (Eds.), *Bayesian Statistics 4*, pp. 169–193. Oxford: Oxford University Press.

Giannone, D., M. Lenza, and G. E. Primiceri (2015). Prior Selection for Vector Autoregressions. *Review of Economics and Statistics 97*(2), 436–451.

Giannone, D. and G. Primiceri (2024). The Drivers of Post-Pandemic Inflation. Technical report, National Bureau of Economic Research.

Giorno, C., P. Richardson, D. Roseveare, and P. van den Noord (1995). Estimating potential output, output gaps and structural budget balances. OECD Economics Department Working Papers 152, OECD Publishing.

Kilian, L. and D. P. Murphy (2012). Why Agnostic Sign Restrictions Are Not Enough: Understanding the Dynamics of Oil Market VAR models. *Journal of the European Economic Association 10*(5), 1166–1188.

Lanne, M. and H. Lütkepohl (2008). Identifying Monetary Policy Shocks via Changes in Volatility. *Journal of Money, Credit and Banking 40*(6), 1131–1149.

Lanne, M., H. Lütkepohl, and K. Maciejowska (2010). Structural Vector Autoregressions with Markov Switching. *Journal of Economic Dynamics and Control 34*(2), 121–131.

Lütkephol, H. (2007). *New Introduction to Multiple Time Series Analysis*. Springer-Verlag.

McKay, A. and R. Reis (2016). The Role of Automatic Stabilizers in the US Business Cycle. *Econometrica 84*(1), 141–194.

Oh, H. and R. Reis (2012). Targeted Transfers and the Fiscal Response to the Great Recession. *Journal of Monetary Economics 59*, S50–S64.

Orchard, J. D., V. A. Ramey, and J. F. Wieland (2025). Micro mpcs and macro counterfactuals: The case of the 2008 rebates. *The Quarterly Journal of Economics 140*(3), 2001–2052.

Parker, J. A., N. S. Souleles, D. S. Johnson, and R. McClelland (2013). Consumer Spending and the Economic Stimulus Payments of 2008. *American Economic Review 103*(6), 2530–53.

Powell, J. H. (2021). Monetary Policy in the Time of COVID. Speech at the Federal Reserve Bank of Kansas City Economic Policy Symposium, Jackson Hole, Wyoming.

Primiceri, G. E. (2005). Time Varying Structural Vector Autoregressions and Monetary Policy. *Review of Economic Studies 72*(3), 821–852.

Raftery, A. E. and S. Lewis (1992). How Many Iterations in the Gibbs Sampler. *Bayesian Statistics 4*(2), 763–773.

Ramey, V. A. (2025). Do Temporary Cash Transfers Stimulate the Macroeconomy? Evidence from Four Case Studies. Working Paper 33503, National Bureau of Economic Research.

Rigobon, R. (2003). Identification through heteroskedasticity. *The Review of Economics and Statistics 85*(4), 777–792.

Romer, C. D. and D. H. Romer (2016). Transfer Payments and the Macroeconomy: The Effects of Social Security Benefit Increases, 1952-1991. *American Economic Journal: Macroeconomics 8*(4), 1–42.

Sentana, E. and G. Fiorentini (2001). Identification, Estimation and Testing of Conditionally Heteroskedastic Factor Models. *Journal of Econometrics 102*(2), 143–164.

Shapiro, A. H. (2024). Decomposing supply and demand driven inflation. Working Paper 2022-18, Federal Reserve Bank of San Francisco.

Shapiro, M. D. and J. Slemrod (2003). Consumer Response to Tax Rebates. *The American Economic Review 93*(1), 381–396.

Shapiro, M. D. and J. Slemrod (2009). Did the 2008 Tax Rebates Stimulate Spending? *American Economic Review 99*(2), 374–79.

Sims, C. A. and T. Zha (2006). Were There Regime Switches in U.S. Monetary Policy? *American Economic Review 96*(1), 54–81.

Summers, L. H. (2022). The Fed Must Do Much More to Fight Inflation—And Fast. Time.

Uhlig, H. (2005). What Are the Effects of Monetary Policy on Output? Results from an Agnostic Identification Procedure. *Journal of Monetary Economics 52*(2), 381–419.